รายงานวิจัยฉบับสมบูรณ์

โครงการการสังเคราะห์สารแอนทราซีน-ฟอสฟีนแอดดักลิแกนด์จากปฏิกิริยา Diels-Alder เพื่อประยุกต์ใช้ในปฏิกิริยาคะตะไลซิสด้วยโลหะพาลลาเดียม เหล็ก และทองแดง

โดย ผศ.ดร. รักเกียรติ จิตคติและคณะ

30 เมษายน 2561

สัญญาเลขที่ MRG5480005

รายงานวิจัยฉบับสมบูรณ์

โครงการการสังเคราะห์สารแอนทราซีน-ฟอสฟีนแอดดักลิแกนด์จากปฏิกิริยา Diels-Alder เพื่อประยุกต์ใช้ในปฏิกิริยาคะตะไลซิสด้วยโลหะพาลลาเดียม เหล็ก และทองแดง

คณะผู้วิจัย

1. **Asst. Dr. Rukkiat Jitchati** chemistry department, faculty of science, Ubon Ratchathani University, THAILAND
2. **Asst. Prof. Dr. Tienthong Thongpanchang**, chemistry department, faculty of science, University, THAILAND
3. **Prof. Dr. Martin R. Bryce**, chemistry department, faculty of science, Durham university, UK

สนับสนุนโดยสำนักงานคณะกรรมการการอุดมศึกษา
สำนักงานกองทุนสนับสนุนการวิจัย และ มหาวิทยาลัยอุบลราชธานี

(ความเห็นในรายงานนี้เป็นของผู้วิจัย สกอ และ สกว. ไม่จำเป็นต้องเห็นด้วยเสมอไป)

บทคัดย่อ

รหัสโครงการ: MRG5480005

ชื่อโครงการ: โครงการการสังเคราะห์สารแอนทราซีน-ฟอสฟีนแอดดักลิแกนด์จากปฏิกิริยา Diels-Alder เพื่อประยุกต์ใช้ในปฏิกิริยาคะตะไลซิสด้วยโลหะพาลลาเดียม เหล็ก และทองแดง

ชื่อนักวิจัย ผศ.ดร.รักเกียรติ จิตคติ. ภาควิชาเคมี คณะวิทยาศาสตร์ มหาวิทยาลัยอุบลราชธานี

อีเมล์: rukkiat_j@hotmail.com

ระยะเวลาโครงการ 2 ปี

บทคัดย่อ

งานวิจัยสังเคราะห์และพิสูจน์เอลักษณ์สารแอนทราซีน-ฟอสฟีนออกไซด์แอดดัก (**L2O**) จากปฏิกิริยา Diels-Alder, phosphenation และ auto oxidation ตามลำดับ นำ **L2O** ที่ได้ไปศึกษาการเป็นลิแกนด์เพิ่มในปฏิกิริยาของ Suzuki–Miyaura cross-coupling และ Sonogashira cross-coupling ที่มีสารเชิงซ้อนของโลหะพาลลาเดียม เหล็ก และทองแดง เป็นตัวเร่ง ได้แก่ $Pd(PPh_3)_2Cl_2$, $FeCl_3$, $Fe(acac)_3$ และ Cu_2O การทดลองพบว่า **L2O** มีความสามารถเป็นลิแกนด์ได้ดีในปฏิกิริยา Suzuki–Miyaura cross-couplings ที่มี $Pd(PPh_3)_2Cl_2$ เป็นตัวเร่งเท่านั้น โดยผลิตภัณฑ์ที่ได้จากปฏิกิริยา Suzuki–Miyaura cross-coupling สามารถนำไปใช้ในการสังเคราะห์สารเชิงซ้อนของโลหะอิริเดียม (III) ชนิดมีประจุ เพื่อนำไปประยุกต์เป็นสารเรืองแสงในเซลล์เรืองแสงด้วยไฟฟ้าชนิดอินทรีย์ที่มีประสิทธิภาพ

คำสำคัญ: ลิแกนด์; แอนทราซีน-ฟอสฟีนออกไซด์แอดดัก; เซลล์เรืองแสงด้วยไฟฟ้าชนิดอินทรีย์; ปฏิกิริยา Suzuki–Miyaura cross-coupling

Abstract

Project Code : MRG5480005

Project Title : Synthesis of Anthracene-phosphineoxide Adduct from Diels-Alder reaction for the palladium, iron and copper catalyst

Investigator : Asst. Dr. Rukkiat Jitchati chemistry department, faculty of science, Ubon Ratchathani University, THAILAND

E-mail Address : rukkiat_j@hotmail.com

Project Period : 2 years

Abstract:

This research synthesized and characterized anthracene-phosphineoxide adduct (**L2O**) as from Diels-Alder, phosphenation and auto oxidation reaction, respectively. **L2O** was used as the additive ligand in Suzuki–Miyaura cross-coupling and Sonogashira cross-coupling by using the complex of palladium, iron and copper specifically, $Pd(PPh_3)_2Cl_2$, $FeCl_3$, $Fe(acac)_3$ and Cu_2O as the catalyst. We found that **L2O** showed the good property only in Suzuki–Miyaura cross-coupling reaction with $Pd(PPh_3)_2Cl_2$ as the catalyst. Furthermore, we used the cross-coupling products as the ligand the synthesis of the charged iridium(III) complexes, which were as the emitter in highly efficient organic light-emitting electrochemical cells (OLECs)

Keywords: Ligand; Anthracene-phosphineoxide adduct; Organic light-emitting electrochemical cells (OLECs); Suzuki-Miyaura cross-coupling reaction

บทสรุปผู้บริหาร (Executive Summary)

ที่มาและความสำคัญของปัญหา

ในอดีตที่ผ่านมา ปฏิกิริยาส่วนใหญ่ของวงเบนซีน (benzene) จะเป็นปฏิกิริยาการแทนที่ด้วยอิเล็กโตรไฟล์ (electrophilic substitution) หรือบางกรณีอาจสามารถเกิดปฏิกิริยาการแทนที่ด้วยนิวคลีโอไฟล์ (nucleophilic substitution) แต่หลังจากการค้นพบปฏิกิริยาการเชื่อมต่อของฟีนอล (phenol) และโบรโมเบนซีน (bromobenzene) โดยใช้โลหะทองแดงเป็นตัวคะตะลีสต์[1] ทำให้งานวิจัยด้านการใช้โลหะทรานสิชันเป็นคะตะลิสต์ ได้รับความสนใจและศึกษากันอย่างกว้างขวางจนกระทั่งปัจจุบัน[2-6] ซึ่งตัวอย่างของปฏิกิริยาการใช้โลหะทรานสิชันเป็นคะตะลิสต์ ในการสังเคราะห์ไบฟีนิล (biphenyl) ได้แก่ ปฏิกิริยา Suzuki-Miyaura, ปฏิกิริยา Stille, ปฏิกิริยา Hiyama, ปฏิกิริยา Negishi, และปฏิกิริยา Kumada เป็นต้น โดยสมการทั่วไปของ transition metal catalyzed coupling reaction สามารถเขียนได้ดังนี้

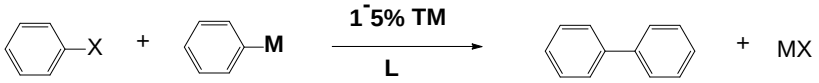

M = B (**Suzuki-Miyaura**)
Sn (Still reaction)
Si (Hiyama reaction)
Zn (Negishi reaction)
Mg (Kumada reaction)

TM = Pd, Cu, Fe, Au, Ni, Ag

L = phosphine, carbene

รูปที่ 1. รูปทั่วไปของปฏิกิริยาคะตะไลซิสด้วยโลหะทรานซีสชันในการสังเคราะห์ไบฟีนิล

นอกจากนี้ยังมีตัวอย่างของปฏิกิริยาการคะตะลิสต์ด้วยโลหะทรานซิชันอย่างอื่น เช่น Buchwald–Hartwig aminations

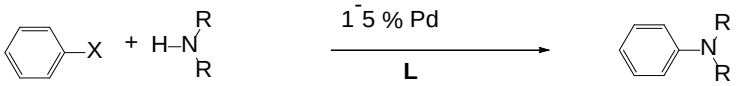

ปฏิกิริยา cyanation[7]

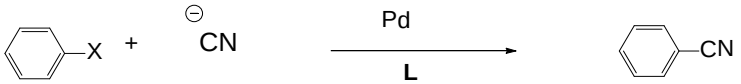

เมื่อต้นปีที่ผ่านมานี้กลุ่มงานวิจัยของมหาวิทยาลัยนิวคาสเซิลได้ทำปฏิกิริยาคะตะไลซิสด้วยสารเชิงซ้อนของโลหะพาลลาเดียมและลิแกนด์แอนทราซีน-ฟอสฟีนแอดดัก (**KITPHOS**) ตามโครงสร้างที่แสดงไว้ในรูปที่ โดยกลุ่มงานวิจัยสามารถทำปฏิกิริยา Buchwald–Hartwig aminations (สมการ 1) และ Suzuki–Miyaura cross-couplings (สมการ 2) ของอนุพันธ์ของวงเบนซีนที่มีความเกะกะสูง และใช้สารเชิงซ้อนของพาลาเดียมเป็นคะตะลิสต์เพียง 0.5 และ 1% ตามลำดับ[8]

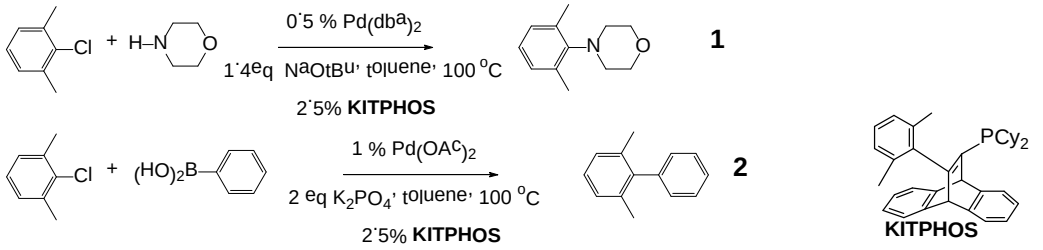

รูปที่ 2. ปฏิกิริยา Buchwald–Hartwig aminations และ Suzuki–Miyaura cross-couplings โดยสารเชิงซ้อนของโลหะพาลลาเดียมและลิแกนด์แอนทราซีน-ฟอสฟีนแอดดัก (**KITPHOS**)

แต่เนื่องจากว่า **KITPHOS** ข้างต้นมีแนวทางการสังเคราะห์ที่ยากและซับซ้อน กลุ่มงานวิจัยของเราจึงมีแนวคิดการสังเคราะห์ลิแกนด์แอนทราซีน-ฟอสฟีนแอดดักชนิดใหม่ที่มีเส้นทางการสังเคราะห์ที่สั้นสง โดยใช้อนุพันธ์ **Y1**[9] เป็นสารตั้งต้นที่สามารถสังเคราะห์ได้ง่ายดังรายงานไว้โดยกลุ่มงานวิจัยของ ศ. ดร. ยอดหทัย เทพธรานนท์

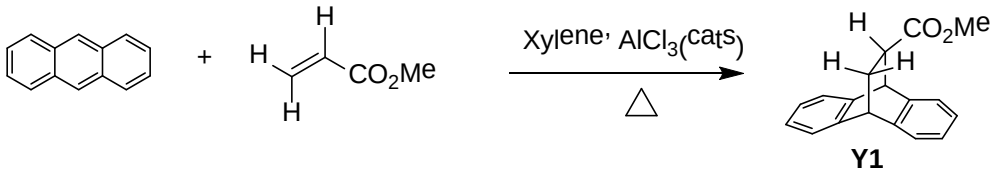

รูปที่ 3. การสังเคราะห์แอนทราซีน-ฟอสฟีนแอดดักโดยกลุ่มงานวิจัยของ ศ. ดร. ยอดหทัย เทพธรานนท์

โดยลิแกนด์แอนทราซีน-ฟอสฟีนแอดดักชนิดใหม่ที่เป็นโมเลกุลเป้าหมายของงานวิจัยนี้จะมีความหลากหลายทางด้านหมู่ฟังชันก์ และความเกะกะ (รูปที่ 4) ยิ่งไปกว่านั้นเรายังแผนที่จะสังเคราะห์ลิแกนด์แอนทราซีน-ฟอสฟีนแอดดักที่มีสมบัติการเบนระนาบแสง (optically active ligand) เพื่อนำไปสังเคราะห์โมเลกุลที่สมบัติเป็น optically active อีกด้วย

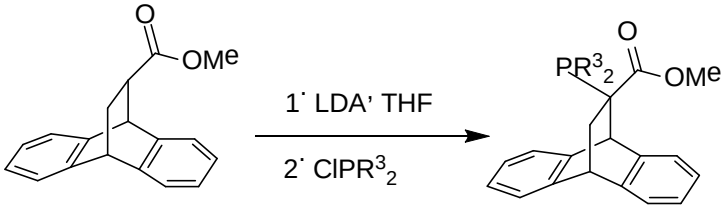

รูปที่ 4. รูปทั่วไปของโมเลกุลเป้าหมายในงานวิจัยนี้

และเมื่อทำการสังเคราะห์แอนทราซีน-ฟอสฟีนแอดดักแล้ว จะนำโมเลกุลฟอสฟีนที่ได้ไปใช้เป็นลิแกนด์ในปฏิกิริยาคะตะไลซิสโดยสารเชิงซ้อนของโลหะพาลลาเดียม, เหล็ก และทองแดง โดยจะทดสอบประสิทธิภาพในปฏิกิริยา Suzuki–Miyaura cross-couplings, Buchwald–Hartwig aminations, cyanation, optically active synthesis, คะตะไลซีสด้วยสารเชิงซ้อนของเหล็ก และคะตะไลซีสด้วยสารเชิงซ้อนของทองแดง ซึ่งจะกล่าวในรายละเอียดต่อไป

วัตถุประสงค์

1. สังเคราะห์โมเลกุลแอนทราซีน-ฟอสฟีนแอดดักชนิดใหม่
2. ทดสอบประสิทธิภาพของลิแกนด์ในปฏิกิริยาคะตะไลซิสโดยใช้สารเชิงซ้อนของโลหะพาลลาเดียม, เหล็ก และทองแดง

แผนการดำเนินงาน

กิจกรรม	**ปีที่ 1**(เดือนที่)					
	1-2	3- 4	5-6	7-8	9-10	11-12
สังเคราะห์และพิสูจน์เอกลักษณ์ของแอนทราซีน-แอดดัก	←	—	—	→		
ทดสอบประสิทธิภาพของลิแกนด์ในปฏิกิริยา Suzuki–Miyaura cross-couplings - โดยใช้สารเชิงซ้อนของพาลลาเดียม - โดยใช้สารเชิงซ้อนของเหล็ก					←	→
	ปีที่ 2(เดือนที่)					
	1-2	3- 4	5-6	7-8	9-10	11-12
ทดสอบประสิทธิภาพของลิแกนด์ในปฏิกิริยา Sonogashira - โดยใช้สารเชิงซ้อนของพาลลาเดียม - โดยใช้สารเชิงซ้อนของเหล็ก - โดยใช้สารเชิงซ้อนของทองแดง	←	—	→			
การสังเคราะห์สารสารเชิงซ้อนของโลหะอิริเดียม (III) ชนิดมีประจุ และนำไปศึกษา OLEDs				←	—	→

ผลการทดลอง

1. สังเคราะห์สารสารแอนทราซีนแอดดัก จากปฏิกิริยา Diels-Alder ของ anthracene และ methyl acrylate ได้สารที่รายงานไว้ก่อนหน้านี้โดย ศ.ดร.ยอดหทัย เทพธรานนท์และคณะ[1]

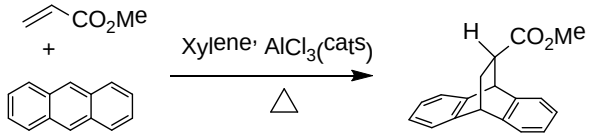

2. สังเคราะห์แอนทราซีน-ฟอสฟีนออกไซด์แอดดัก จากปฏิกิริยา phosphenation แล้วตามด้วย auto oxidative ในบรรยากาศปกติ

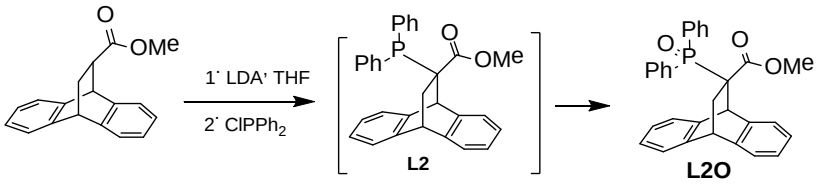

white solid (36% yield); m.p. 206-208 ^{o}C; ^{1}H NMR ($CDCl_3$, 300 MHz): □ 2.47 (ddd, *J* = 21, 15, 3 Hz, 1H), 2.94 (ddd, *J* = 15, 9, 3 Hz, 1H), 3.10 (s, 3H), 4.31 (s, 1H), 3.56 (d, *J* = 6 Hz, 1H), 7.03-7.28 (m, 13H), 7.53-7.56 (m, 3H) 7.85-7.91 (m, 2H); ^{13}C NMR ($CDCl_3$, 75 MHz): □ 33.8, 44.0, 49.6, 52.3, 58.1, 58.8, 123.0, 123.6, 124.1, 125.7, 125.8,126.5, 126.7, 126.9, 127.7, 127.9, 128.1, 128.2, 131.1, 131.7, 131.8, 131.9, 132.0, 138.8, 140.6, 140.7, 143.9, 144.7, 171.7; IR(KBr) 536, 694, 706, 1193, 1217, 1434, 1732, 2946, 2960 cm^{-1}; MS (ESI) 465.09 (MH^+, 100%).

3. การทดสอบความเป็นลิแกนด์ L2O ในปฏิกิริยา Suzuki–Miyaura cross-couplings โดยใช้ $Pd(PPh_3)_2Cl_2$ (1 mol%) เป็นตัวเร่งปฏิกิริยา, phenyl boronic acid (3.51 mmol), 2-chloropyridine (3.51 mmol), base (8.75 mmol), solvent (20 ml) เป็นเวลา 6 ชั่วโมง ผลดังตารางที่ 1

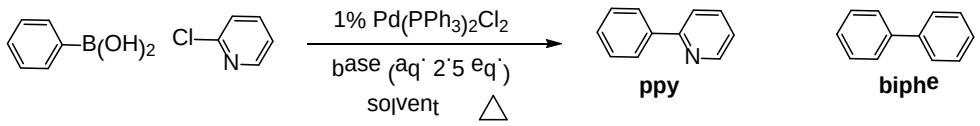

ตารางที่ 1 Optimization of the Pd(II)-catalyzed reaction of phenyl boronic acid and 2-chloropyridine

Entry	Base	Solvent	Temp (^{o}C)	Ligand	**ppy/Clpy** (peak area ratio) [a]	**ppy/biphe** (peak area ratio) [a]
1	1 M Na_2CO_3 (aq.)	THF	65	-	0.1	1.2
2	1 M Na_2CO_3 (aq.)	THF	65	10% **L2O**	1.7	23.6
3	1 M Na_2CO_3 (aq.)	THF	65	10% PPh_3	1.0	19.7
4	1 M NaOH (aq.)	THF	65	10% PPh_3	0.04	0.5
5	1 M Na_2CO_3 (aq.)	THF	65	10% **phen**	0.04	0.3
6	1 M NaOH (aq.)	THF	65	10% **L2O**	0.002	0.4
7	1 M Na_2CO_3 (aq.)	THF	65	10% dppf	0.71	175.9
8	1 M Na_2CO_3 (aq.)	THF	65	10% dppe	0.03	0.15
9	Na_2CO_3 (s)	THF	65	10% **L2O**	0.53	5.35
10	1 M Na_2CO_3 (aq.)	1,4-dioxane	101	10% **L2O**	>1000	54.7

[a] ratio determine by GC and calculated from peak area.

จากตารางที่ 1 พบว่า ลิแกนด์ แอนทราซีน-ฟอสฟีนออกไซด์แอดดัก (L2O) ดีที่สุด สามารถเร่งปฏิกิริยา Suzuki–Miyaura cross-couplings ได้ดีที่สุด (Entry 10) และเมื่อนำไปสังเคราะห์สารเป้าหมายดังรายงานไว้ใน

ตารางที่ 2 พบว่าสามารถสังเคราะห์ได้ทั้งกับ electron-rich thiophene boronic acid (Entry 2) และ electron poor (2,4-difluorobenzene) boronic acids (Entry 3) ยิ่งไปกว่านั้น ใช้ได้กับ bulky mesitylboronic acid (Entry 6) และยังสามารถนำมาสังเคราะห์กับ less reactive, mono- and dibromo phenanthroline อีกด้วย (Entry 7-8)

Table 2. Pd(II)-catalysed cross-coupling Suzuki-Miyaura reaction of aryl boronic acid and aryl halide[a]

Entry	Aryl halide	Aryl boronic acid	Product	% Yield[b]
1	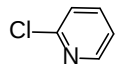	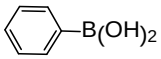	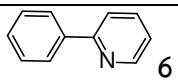 **6**	70
2	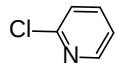	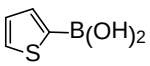	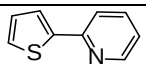 **8**	60
3	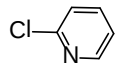	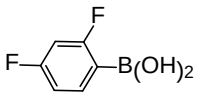	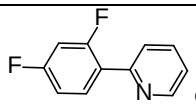 **9**	71
4	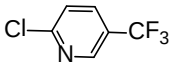	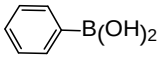	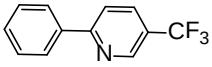 **10**	85
5		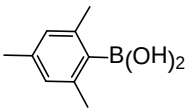	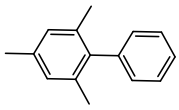 **11**	45
6	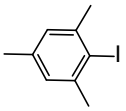	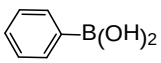	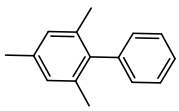 **11**	62
7	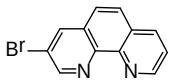	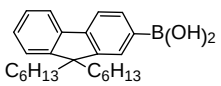	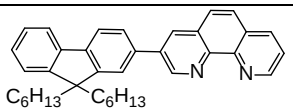 **12**	65
8[c]	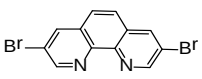	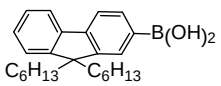	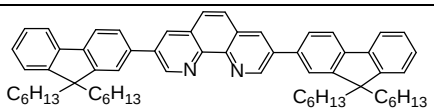 **13**	54

[a] Reaction conditions: $PdCl_2(PPh_3)_2$ (1% mol, 0.035 mmol), **P2O** (10% mol, 0.35 mmol), aryl boronic acid (3.51 mmol), aryl halide (3.51 mmol), 1 M Na_2CO_3 (8.75 mmol) in refluxing 1,4-dioxane (20 mL) for 4 hours; [b] yield of purified product; [c] aryl boronic acid (7.2 mmol)

2-Phenyl pyridine (**6**); colourless liquid; ^{1}H NMR (300 MHz, $CDCl_3$) δ 8.70 (s, 1H), 8.00 (d, *J* = 7.0 Hz, 2H), 7.74 (s, 2H), 7.55–7.38 (m, 4H), 7.24 (d, *J* = 6.4 Hz, 1H); ^{13}C NMR (75 MHz, $CDCl_3$) □ 157.6,

149.5, 139.4, 136.8, 128.9, 128.7, 126.9, 122.1, 120.5; IR(NaCl) 692, 746, 800, 920, 993, 1020, 1076, 1152, 1292, 1423, 1449, 1465, 1587, 1960, 2358, 2857, 2929, 3064 cm^{-1}.

2-Thionyl pyridine (8); white solid; m.p. 59-61 ^{o}C; ^{1}H NMR (300 MHz, $CDCl_3$) □ 8.57 (d, *J* = 4.8 Hz, 1H), 7.78–7.63 (m, 3H), 7.59 (d, *J* = 3.5 Hz, 1H), 7.40 (d, *J* = 5.2 Hz, 1H), 7.20–7.07 (m, 2H); ^{13}C NMR (75 MHz, $CDCl_3$) □ 152.6, 149.5, 136.6, 131.9, 130.8, 128.7, 128.0, 127.5, 124.5, 121.9, 118.78; IR(NaCl) 710, 779, 992, 1155, 1435, 1464, 1580, 3030 cm^{-1}.

2,4-Difluorophenyl pyridine (**9**); colourless liquid; ^{1}H NMR (300 MHz, $CDCl_3$) □ 8.70 (d, *J* = 4.8 Hz, 1H), 7.99 (dd, *J* = 15.7, 8.6 Hz, 1H), 7.74 (d, *J* = 3.8 Hz, 2H), 7.24 (dd, *J* = 8.8, 4.5 Hz, 1H), 7.05–6.96 (m, 1H), 6.91 (t, *J* = 10.0 Hz, 1H); ^{13}C NMR (75 MHz, $CDCl_3$) □ 163.7 (dd, *J* = 253.0, 12.0 Hz), 160.1 (dd, *J* = 253.0, 12.0 Hz), 152.6 (d, *J* = 3.0 Hz), 149.8 (s), 136.4 (s), 132.1 (dd, *J* = 10.0, 4.0 Hz), 124.2 (d, *J* = 10.0 Hz), 123.9–123.6 (m), 122.4 (s), 111.8 (dd, *J* = 21.1, 3.7 Hz), 104.33 (dd, *J* = 27.0, 25.4 Hz); IR(NaCl) 456, 514, 563, 586, 749, 780, 855, 970, 1107, 1144, 1264, 1502, 1613, 2924, 3070 cm^{-1}.

5-(Trifluoromethyl)-2-phenylpyridine (**10**); white solid; m.p. 60-62 ^{o}C; ^{1}H NMR (300 MHz, $CDCl_3$) □ 8.96 (s, 1H), 8.04 (dd, *J* = 7.6, 1.7 Hz, 2H), 7.99 (dd, *J* = 8.4, 1.9 Hz, 1H), 7.85 (d, *J* = 8.3 Hz, 1H), 7.56–7.47 (m, 3H); ^{13}C NMR (75 MHz, $CDCl_3$) □ 160.3 (s), 146.5 (dd, *J* = 13.7, 9.2 Hz), 137.9 (s), 134.1–133.8 (m), 130.6–129.8 (m), 128.9 (s), 129.3–125.3 (m), 127.2 (s), 124.7–120.4 (m), 119.9 (s); IR(NaCl) 693, 741, 790, 839, 861, 1012, 1088, 1123, 1335, 1603, 2929, 3100 cm^{-1}.

Trimethylphenylbenzene (**11**); colourless liquid; ^{1}H NMR (300 MHz, $CDCl_3$) □ 7.70 (t, *J* = 7.3 Hz, 2H), 7.61 (t, *J* = 7.3 Hz, 1H), 7.46 (d, *J* = 7.0 Hz, 2H), 7.26 (s, 2H), 2.66 (s, 3H), 2.35 (s, 6H); ^{13}C NMR (75 MHz, $CDCl_3$) □ 141.2, 139.2, 136.6, 136.0, 129.4, 128.5, 128.2, 126.6, 21.1, 20.8.

3-(9,9-Dihexyl-9H-fluoren-2-yl)-1,10-phenanthroline (**12**); viscous liquid; ^{1}H NMR (300 MHz, $CDCl_3$) □ 7.72 (d, *J* = 6.9 Hz, 2H), 7.58 (dd, *J* = 14.6, 7.9 Hz, 2H), 7.42–7.24 (m, 9H), 6.87–6.77 (m, 2H), 2.04–1.87 (m, 4H), 1.21–0.97 (m, 12H), 0.78 (t, *J* = 6.7 Hz, 6H), 0.71–0.62 (m, 4H); ^{13}C NMR (75 MHz, $CDCl_3$) □ 155.3, 153.0, 150.7, 150.1, 141.1, 141.0, 134.3, 126.9, 126.6, 125.9, 122.8, 122.6,

120.5, 119.6, 118.7, 113.9, 110.1, 55.0, 55.1, 40.5, 40.4, 31.5, 31.4, 29.7, 29.6, 23.7, 23.6, 22.6, 22.5, 13.9; IR(NaCl) 741, 895, 1102, 1376, 1420, 1460, 2369, 2929, 3036 cm^{-1}.

3,8-bis(9,9-dihexyl-9H-fluoren-2-yl)-1,10-phenanthroline (**13**): ^{1}H NMR ($CDCl_3$, 300 MHz): □ 0.75-0.81 (m, 20H), 1.00-1.27 (m, 24H), 2.06-2.09 (m, 8H), 7.36-7.42 (m, 5H), 7.71-7.81 (m, 5H), 7.90 (dd, *J* = 9, 6 Hz, 2H), 7.97 (t, *J* = 6 Hz, 2H), 8.45-8.50 (m, 3H), 9.23 (d, *J* = 3 Hz, 1H), 9.52 (d, *J* = 3 Hz, 1H), 9.54 (d, *J* = 0.5 Hz, 1H); ^{13}C NMR ($CDCl_3$, 75 MHz): □□14.0, 22.5, 23.8, 29.7, 31.5, 40.3, 55.3, 119.7, 120.0, 120.4, 121.8, 123.0, 125.9, 126.5, 126.9, 127.0, 127.6, 128.2, 128.5, 129.6, 133.3, 136.0, 136.8, 137.5, 140.3, 140.4, 141.5, 141.7, 144.5, 149.7, 150.0, 151.1, 151.3, 152.0; IR(KBr) 541, 741, 1120, 1171, 1335, 1414, 1609, 2856, 2927, 3064, 3210 cm^{-1}.

4. การทดสอบความเป็นลิแกนด์ L2O ในปฏิกิริยา Suzuki–Miyaura cross-couplings โดยใช้ $FeCl_3$ (10 mol%) เป็นตัวเร่งปฏิกิริยา $FeCl_3$, phenylboronic acid (1.9305 mmol), 2-chloropyridine (1.755 mmol), เบส (6.1425 mmol), ตัวทำละลาย EtOH (15 mL) ดังรายงานในตารางที่ 3

ตารางที่ 3 ผลการทดลองปฏิกิริยา Suzuki-Miyaura cross-coupling ระหว่าง 2-chloro pyridine กับ phenylboronic acid ด้วย $FeCl_3$

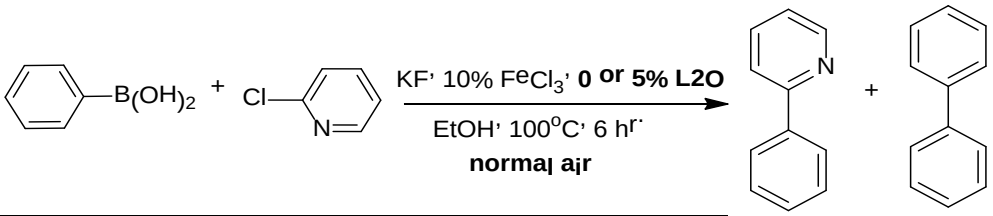

entry	% **L2O**	%Cross-coupling	%Homo- coupling
1	0	0	0
2	5%	0	0

จากการทดลองพบว่า ลิแกนด์ **L2O** ไม่สามารถช่วยเร่ง ปฏิกิริยา Suzuki-Miyaura cross-coupling ด้วย $FeCl_3$

5. การทดสอบความเป็นลิแกนด์ L2O ในปฏิกิริยา Sonogashira cross-coupling โดยใช้ $Pd(PPh_3)_2Cl_2$ (1 mol%) เป็นตัวเร่งปฏิกิริยา ใช้ phenylacetylene (1.1 eq) กับ bromobenzene (1 eq) ใช้ 1% Pd(II), เบส 2.5 eq, CuI (0.005 eq), %5 L2O ลิแกนด์ ใช้ 1,4-dioxane เป็นตัวทำละลาย ดังรายงานในตารางที่ 4

ตารางที่ 4 ผลการทดลองปฏิกิริยา Sonogashira cross-coupling ระหว่าง phenylacetylene กับ bromobenzene โดยใช้ $Pd(PPh_3)_2Cl_2$

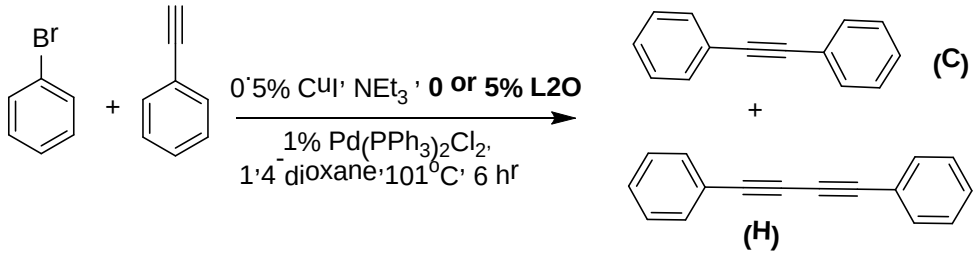

entry	สภาวะ	% **L2O**	%Cross-coupling (**C**) [a]	Homo- coupling (**H**) [a]
1	N_2	0	1	0.37
2	N_2	5%	2	0.20
3	บรรยากาศปกติ	0	5**	0.32**
4	บรรยากาศปกติ	5%	1	0.29

[a] คำนวณจากพื้นที่ใต้กราฟของเทคนิค GC เทียบกับ dodecane

จากการทดลองพบว่า ลิแกนด์ **L2O** ช่วยให้เกิดปฏิกิริยา Sonogashira cross-coupling ในสภาวะ $Pd(PPh_3)_2Cl_2$ (1 mol%) เป็นตัวเร่งปฏิกิริยาได้เพียง 5 %

6. การทดสอบความเป็นลิแกนด์ L2O ในปฏิกิริยา Sonogashira cross-coupling โดยใช้ $FeCl_3$ (15 mol%) เป็นตัวเร่งปฏิกิริยา, phenylboronic acid (1.9305 mmol), 2-chloropyridine (1.755 mmol), เบส (2.5476 mmol), ตัวทำละลาย toluene (15 mL) รายงานไว้ใน ตารางที่ 5

ตารางที่ 5 ผลการทดลองปฏิกิริยา Sonogashira cross-coupling ระหว่าง phenylacetylene กับ bromobenzene ด้วย $FeCl_3$

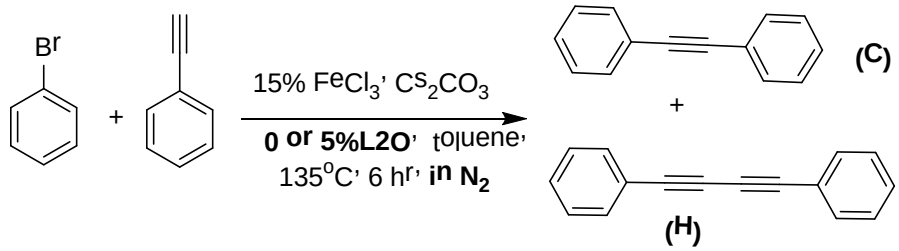

entry	% L2O	%Cross-coupling (C) [a]	Homo- coupling (H) [a]
1	0	0	0
2	5%	0	0

[a] คำนวณจากพื้นที่ใต้กราฟของเทคนิค GC เทียบกับ dodecane

จากการทดลองพบว่า ลิแกนด์ L2O ไม่สามารถช่วยเร่ง ในปฏิกิริยา Sonogashira cross-coupling ในสภาวะ $FeCl_3$ (15 mol%) เป็นตัวเร่งปฏิกิริยา

7. การศึกษาสภาวะที่เหมาะสมของลิแกนด์ L2O ในปฏิกิริยา Sonogashira cross-coupling โดยใช้ $Fe(acac)_3$ (30 mol%) เป็นตัวเร่งปฏิกิริยา, phenylboronic acid (1.9305 mmol), 2-chloropyridine (1.755 mmol), เบส (2.5476 mmol), copper(I) iodide (0.1274 mmol), ตัวทำละลาย DMSO (7 ml) แสดงผลใน

ตารางที่ 6 ผลการทดลองปฏิกิริยา Sonogashira cross-coupling ระหว่าง phenylacetylene กับ bromobenzene โดยใช้ $Fe(acac)_3$

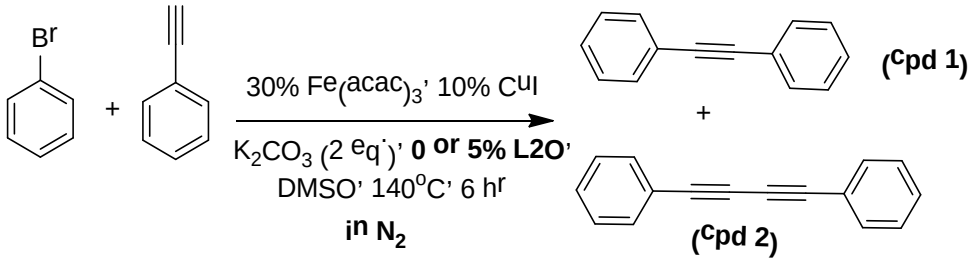

entry	สภาวะ	% L2O	%Cross-coupling	Homo- coupling[a]
1	N_2	0	1	0.02
2	N_2	5%	0	0.09

[a] คำนวณจากพื้นที่ใต้กราฟของเทคนิค GC

จากการทดลองพบว่า ลิแกนด์ L2O ไม่สามารถช่วยเร่ง ในปฏิกิริยา Sonogashira cross-coupling โดยใช้ $FeCl_3$ เป็นตัวเร่งปฏิกิริยา

8. การศึกษาสภาวะที่เหมาะสมของลิแกนด์ L2O ในปฏิกิริยา Sonogashira cross-coupling โดยใช้ Cu_2O (2 mol%) เป็นตัวเร่งปฏิกิริยา, phenylboronic acid (1.9305 mmol), 2-chloropyridine (1.755 mmol), เบส (2.5476 mmol),ตัวทำละลาย 1,4-dioxane (15 mL) แสดงผลในตารางที่ 7

ตารางที่ 7 ผลการทดลองปฏิกิริยา Sonogashira cross-coupling ระหว่าง phenylacetylene กับ bromobenzene โดยใช้ **Cu_2O**

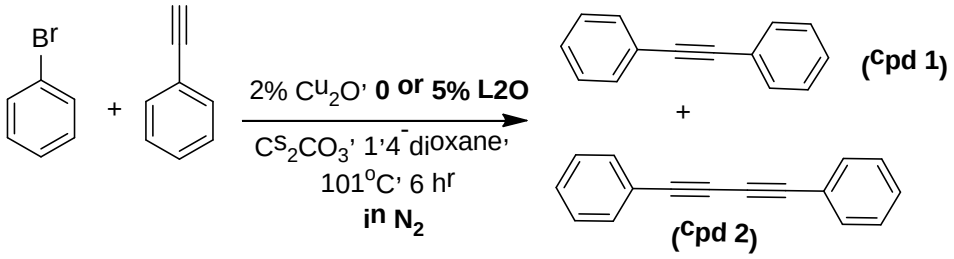

entry	สภาวะ	% **L2O**	%Cross-coupling [a]	Homo- coupling[a]
1	N_2	0	0	0
2	N_2	5%	0	0

[a] คำนวณจากพื้นที่ใต้กราฟของเทคนิค GC เทียบกับ dodecane

จากการทดลองพบว่า ลิแกนด์ **L2O** ไม่สามารถช่วยเร่ง ในปฏิกิริยา Sonogashira cross-coupling โดยใช้ Cu_2O เป็นตัวเร่งปฏิกิริยา

จากการทดลองในข้างต้นพบว่า สารแอนทราซีน-ฟอสฟีนออกไซด์แอดดัก **L2O** เหมาะในปฏิกิริยา **Suzuki–**Miyaura cross-couplings ที่มี $PdCl_2(PPh_3)_2$ เป็นตัวเร่ง จึงนำไปสังเคราะห์สารสารเชิงซ้อนของโลหะอิริเดียม (III) ชนิดมีประจุ ต่อไป

8. การสังเคราะห์สารสารเชิงซ้อนของโลหะอิริเดียม (III) ชนิดมีประจุ โดยใช้สาร **6** ในตางรางที่ 2 ที่เพื่อสังเคราะห์ **Complex 1- 5**

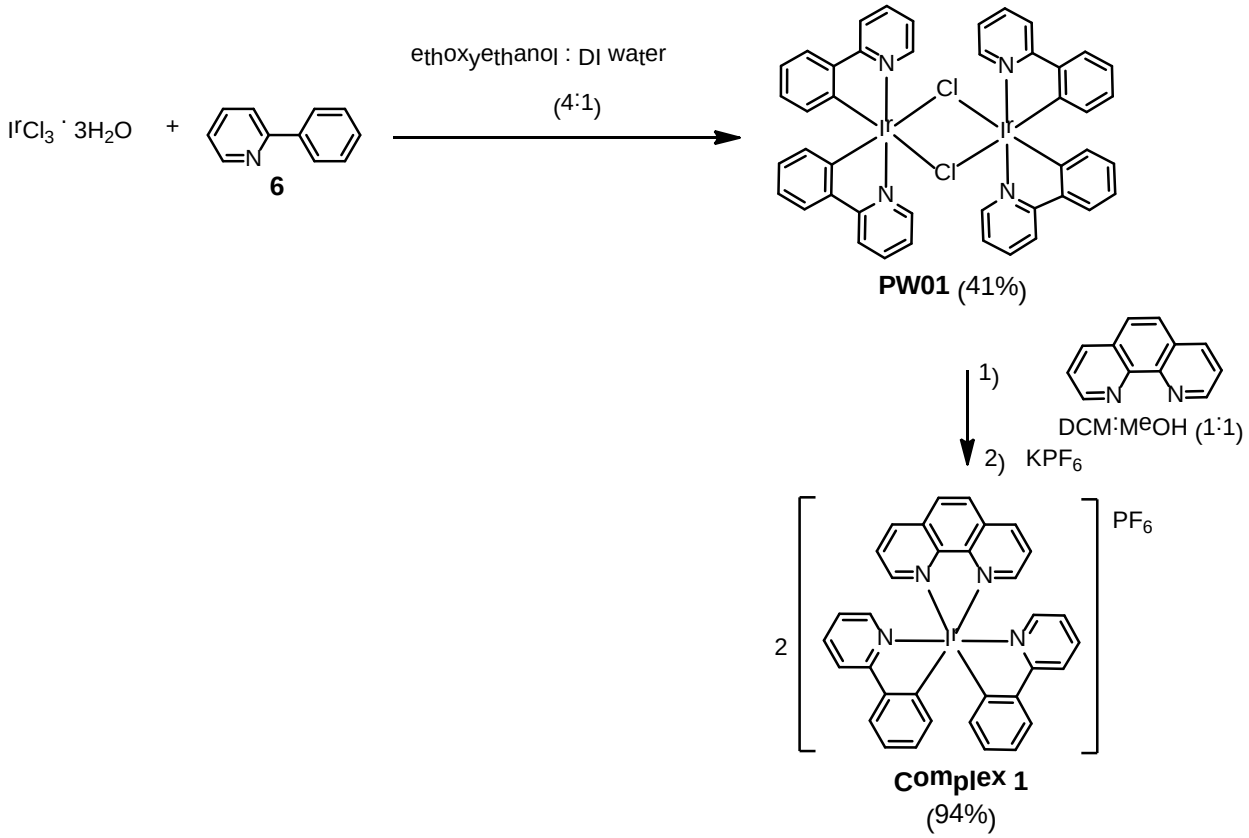

ในแนวทางเดียวกันเราสามารถสังเคราะห์ **Complex 2-5** ที่มีโครงสร้างดังต่อไปนี้

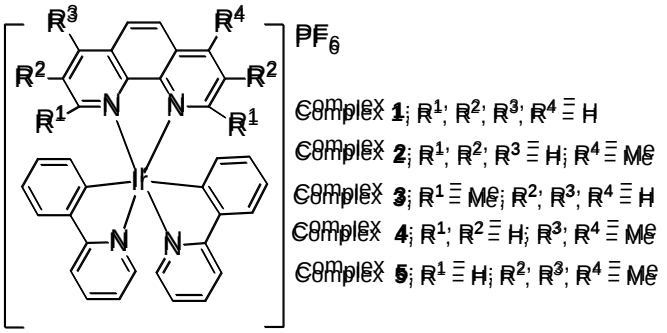

{(1,10-Phenanthroline-N-N′)- bis-(2-phenylpyridine-C$^{2'}$,N)-iridium(III) hexafluorophosphate)complex 1( )0.15 g, 94 %(, ^{1}H NMR (300 MHz, acetone-D_6) □ 8.90 (d, *J* = 8.2 Hz, 1H), 8.51 – 8.32

(m, 2H), 8.23 (d, *J* = 8.1 Hz, 1H), 8.07 (dd, *J* = 8.2, 5.0 Hz, 1H), 7.90 (dd, *J* = 15.7, 7.9 Hz, 2H), 7.67 (d, *J* = 5.5 Hz, 1H), 7.07 (t, *J* = 7.5 Hz, 1H), 6.96 (dd, *J* = 8.7, 4.6 Hz, 2H), 6.45 (d, *J* = 7.4 Hz, 1H); ^{13}C NMR (75 MHz, acetone-D_6) □ 167.81, 151.27, 149.87, 149.37, 146.93, 144.29, 138.75, 138.55, 131.79, 131.71, 130.32, 128.45, 126.99, 124.90, 123.43, 122.56, 119.81; Ms (ES^+): m/z(%) 681.1630 (M^+-PF_6, 100).

{(4-Methyl-1,10-phenanthroline-N-N′)- bis-(2-phenylpyridine-$C^{2'}$,N)-iridium(III)} hexafluorophosphate) complex 2( )0.08 g, 49 %(, ^{1}H NMR (300 MHz, acetone-D_6) □ 8.86 (d, *J* = 8.2 Hz, 1H), 8.50 (d, *J* = 9.1 Hz, 1H), 8.40 (t, *J* = 7.4 Hz, 2H), 8.23 (dd, *J* = 13.2, 6.7 Hz, 3H), 8.01 (dd, *J* = 8.2, 5.1 Hz, 1H), 7.88 (dd, *J* = 14.3, 7.1 Hz, 5H), 7.66 (d, *J* = 5.6 Hz, 2H), 6.99 (ddd, *J* = 18.5, 14.8, 7.3 Hz, 6H), 6.54 – 6.36 (m, 2H), 2.99 (s, 3H); ^{13}C NMR (75 MHz, $CDCl_3$) □ 205.44, 167.84, 167.80, 151.25, 150.44, 150.27, 149.27, 149.23, 147.03, 146.50, 144.35, 144.28, 138.64, 138.52, 131.84, 131.79, 131.46, 131.30, 130.29, 128.09, 127.52, 126.85, 125.09, 124.89, 123.46, 123.44, 122.47, 119.80, 18.22; Ms (ES^+): m/z(%) 740.1618 (M^+-PF_6+2Na^+, 100).

{(2,9-Dimethyl-1,10-phenanthroline-N-N′)- bis-(2-phenylpyridine-$C^{2'}$,N)-iridium(III)} hexafluorophosphate (complex 3))0.145 g, 91 %(, ^{1}H NMR (300 MHz, $CDCl_3$) □ 8.72 (d, *J* = 8.3 Hz, 1H), 8.23 (t, *J* = 3.7 Hz, 2H), 7.92 (t, *J* = 7.8 Hz, 1H), 7.82 (t, *J* = 6.9 Hz, 3H), 7.01 (t, *J* = 6.6 Hz, 1H), 6.95 (t, *J* = 7.6 Hz, 1H), 6.79 (t, *J* = 7.4 Hz, 1H), 6.21 (d, *J* = 7.6 Hz, 1H), 2.21 (s, 3H); ^{13}C NMR (75 MHz, acetone-D_6) □ 205.34, 205.07, 167.85, 165.19, 150.15, 148.95, 148.00, 143.48, 139.22, 138.50, 131.57, 130.04, 129.71, 128.03, 127.24, 124.82, 123.04, 122.10, 119.80, 26.8; Ms (ES^+): m/z(%) 709.1943 (M^+-PF_6, 100).

{(4,7-Dimethyl-1,10-phenanthroline-N-N′)- bis-(2-phenylpyridine-$C^{2'}$,N)-iridium(III)} hexafluorophosphate (complex 4)) 0.15 g, 94 %(, ^{1}H NMR (300 MHz, $CDCl_3$) □ 8.24 (s, 1H), 8.08 (d, *J* = 5.1 Hz, 1H), 7.87 (d, *J* = 8.1 Hz, 1H), 7.74 – 7.58 (m, 2H), 7.52 (d, *J* = 5.1 Hz, 1H), 7.34 (d, *J* = 5.5 Hz, 1H), 7.04 – 6.79 (m, 3H), 6.39 (d, *J* = 7.3 Hz, 1H), 2.85 (s, 3H); ^{13}C NMR (75 MHz, $CDCl_3$) δ 167.72, 150.33, 150.16, 148.94, 148.56, 146.45, 143.85, 138.16, 131.93, 131.03, 130.62, 127.23, 124.73, 123.40, 122.53, 119.58, 19.04; Ms (ES^+): m/z(%) 709.1943 (M^+-PF_6, 100).

{(3,4,7,8-Tetramethyl-1,10-phenanthroline-N-N′)- bis-(2-phenylpyridine-$C^{2'}$,N)-iridium(III)} hexafluorophosphate (complex 5))0.15 g, 92 %(; ^{1}H NMR (300 MHz, $CDCl_3$) □ 8.26 (s, 1H), 7.91 (s, 1H), 7.89 (d, *J* = 8.3 Hz, 1H), 7.68 (t, *J* = 6.9 Hz, 2H), 7.36 (d, *J* = 5.6 Hz, 1H), 7.02 (t, *J* = 7.1 Hz,

1H), 6.92 (dd, *J* = 10.6, 6.1 Hz, 2H), 6.38 (d, *J* = 7.3 Hz, 1H), 2.78 (s, 3H), 2.36 (s, 3H); ^{13}C NMR (75 MHz, $CDCl_3$) □ 167.80, 151.03, 150.60, 148.70, 146.38, 145.41, 143.74, 137.88, 135.06, 131.88, 130.67, 130.02, 124.63, 124.42, 123.31, 122.42, 119.41, 18.07, 14.99; Ms (ES^+): m/z(%) 737.2256 (M^+-PF_6, 100).

เอกสารอ้างอิง

(1) Siwapinyoyos, T.; Thebtaranonth, Y. *J. Org. Chem.* **1982**, *47*, 598.

(2) Costa, R. D.; Orti, E.; Bolink, H. J.; Graber, S.; Schaffner, S.; Neuburger, M.; Housecroft, C. E.; Constable, E. C. *Adv. Funct. Mater.* **2009**, *19*, 3456.

(3) Lowry, M. S.; Hudson, W. R.; Pascal, R. A.; Bernhard, S. *J. Am. Chem. Soc.* **2004**, *126*, 14129.

(4) Rothe, C.; Chiang, C.-J.; Jankus, V.; Abdullah, K.; Zeng, X.; Jitchati, R.; Batsanov, A. S.; Bryce, M. R.; Monkman, A. P. *Adv. Funct. Mater.* **2009**, *19*, 2038.

(5) Moon, D. B.; Choe, Y. S. *Mol. Cryst. Liq. Cryst.* **2013**, *584*, 60.

(6) Dragonetti, C.; Falciola, L.; Mussini, P.; Righetto, S.; Roberto, D.; Ugo, R.; Valore, A.; DeAngelis, F.; Fantacci, S.; Sgamellotti, A.; Ramon, M.; Muccini, M. *Inorg. Chem.* **2007**, *46*, 8533.

Output จากโครงการวิจัยที่ได้รับทุนจาก สกว.

ผลงานตีพิมพ์ในวารสารวิชาการนานาชาติ

1. P. Wongkaew, U. Mahanitipong, N. Wongsang, S. Sahasithiwat, **R. Jitchati**, Highly Efficient Light-Emitting Electrochemical Cells (LECs) from Host-Guest Cationic Iridium(III) Complexes, e-J. Surf. Sci. Nanotech., **12** (2014) 141-144.

2. P. Li, G.-G. Shan, H.-T. Cao, D.-X. Zhu, Z.-M. Su, **R. Jitchati**, M. R. Bryce, Intramolecular **π** Stacking in Cationic Iridium(III) Complexes with Phenyl-Functionalized Cyclometalated Ligands: Synthesis, Structure, Photophysical Properties, and Theoretical Studies, Eur. J. Inorg. Chem., **2014** (2014) 2376–2382.

3. K. Wongkhana, U. Mahanitiponga, M. Srikaewa, Y. Tantirunggrotchaib, S. Sahasithiwatc, R. Jitchati Highly efficient Blue LECs Using Charged Iridium Complexes ACTA PHYSICA POLONICA A (2015) 1019-1011.

Appendix

e-Journal of Surface Science and Nanotechnology 5 April 2014

e-J. Surf. Sci. Nanotech. Vol. 12 (2014) 141-144 Conference - ACSIN-12&ICSPM21 -

Highly Efficient Light-Emitting Electrochemical Cells (LECs) from Host-Guest Cationic Iridium(III) Complexes*

Praweena Wongkaew, Usana Mahanitipong, and Natsiri Wongsang
Center for Organic Electronic and Alternative Energy (COEA), Department of Chemistry, Faculty of Science, Ubon Ratchathani University, Warinchumrap, Ubon Ratchathani Province, 34190, Thailand

Somboon Sahasithiwat
National Metal and Materials Technology Center, Thailand Science Park, Pathumthani, Bangkok, 12110, Thailand

Rukkiat Jitchati†
Center for Organic Electronic and Alternative Energy (COEA), Department of Chemistry, Faculty of Science, Ubon Ratchathani University, Warinchumrap, Ubon Ratchathani Province, 34190, Thailand.
(Received 14 January 2014; Accepted 14 February 2014; Published 5 April 2014)

Five charged iridium(III) complexes with a different number and position of methyl group; $[Ir(phen)(ppy)_2]PF_6$ (**1**), $[Ir(4\text{-phen})(ppy)_2]PF_6$ (**2**), $[Ir(2,9\text{-phen})(ppy)_2]PF_6$ (**3**), $[Ir(4,7\text{-phen})(ppy)_2]PF_6$ (**4**) and $[Ir(4,5/6,7\text{-phen})(ppy)_2]PF_6$ (**5**) were synthesized and characterized by NMR, IR, UV-Vis absorption, fluorescence spectroscopy and cyclic voltammetry. The host-guest light-emitting electrochemical cells (LECs) based on ITO/PEDOT:PSS/**1-5**:PVK (1:4)/Al were investigated, which resulted in a maximum current efficiency at 1.35 cdA^{-1} and a brightness at 717 cdm^{-2} from **5**. The host-guest LECs can be improved by the insertion of the TPBi and LiF layers. We found that the highly efficient electroluminescence device gave the peak current efficiency to 4.49 cdA^{-1}, the maximum brightness at 1,200 cdm^{-2} with Commission Internationale de L'Eclairage (CIE) coordinates of (0.30, 0.54) from **3**. [DOI: 10.1380/ejssnt.2014.141]

Keywords: Iridium; Nano-electronics and related devices; Nano-films; Nano-materials

I. INTRODUCTION

The charged iridium(III) complexes have been studied for advanced optoelectronic applications [1–4]. The advantages of these complexes are their high stabilities, high luminescence quantum yields, short excited state lifetime and tunable emission energies. Its structure compose of one N,N bidentate and two C,N bidentate ligands. The photophysical properties of these phosphors can be tuned by varying both N,N and C,N ligands [5]. Organic light-emitting diodes (OLEDs) and light-emitting electrochemical cells (LECs) have been made and studied during recent years motivated due to their potentially in display technology applications to replace LED technologies [6–8]. The charged Ir(III) complexes have been used as the emitter in both OLED and simple LEC devices [9]. Single layer LECs based on a charged iridium(III) shown by Youngson give high luminescence at 5199 and 4751 cdm^{-2} [10]. Lian and Yong demonstrated an efficient red emitting host-guest LEC based on cationic iridium complexes. The host-guest LEC has brightness of 8.4 cdm^{-2}, external quantum efficiency (EQE) of up to 3.5% and peak current efficiency of 3.4 cdA^{-1} [11]. Recently, Yong Qiu demonstrated a warm-white light LECs with the peak external quantum efficiency, current efficiency, and power efficiency reach 5.2%, 11.2 cdA^{-1}, and 10 lmW^{-1} [12]. In this article, we show the highly efficient host-guest OLED devices based on a charged iridium(III) complex by the insertion of the TPBi and LiF layers.

II. EXPERIMENTAL

All chemicals were purchased from Acros organic and used without further purification, unless otherwise noted. The following five charged iridium(III) complexes (**1-5**) were synthesized according to the reference by varying the N,N ligands [13]. ^{1}H and ^{13}C NMR spectra were recorded on a Bruker Avance 300 spectrometer. Chemical shifts are quoted downfield from internal standard TMS. MS data were obtained using a Thermo Finnigan LTQFT instrument. Ultraviolet-visible (UV-vis) spectra were recorded with Perkin-Elmer UV Lambda 25. Photoluminescence spectrum and the fluorescence quantum yield were identified by a Perkin-Elmer LS 50B Luminescence Spectrometer the standard quinine sulfate solution in 0.01 M H_2SO_4, whose fluorescence quantum yield is known to be 0.54.

(1) {(1,10-Phenanthroline-N-N′)-bis-(2-phenylpyridine-C$^{2'}$,N)-iridium(III)}hexafluorophosphate: (0.15 g, 94%), ^{1}H NMR (300 MHz, acetone-D_6) δ 8.90 (d, J = 8.2 Hz, 1H), 8.51-8.32 (m, 2H), 8.23 (d, J = 8.1 Hz, 1H), 8.07 (dd, J = 8.2, 5.0 Hz, 1H), 7.90 (dd, J = 15.7, 7.9 Hz, 2H), 7.67 (d, J = 5.5 Hz, 1H), 7.07 (t, J = 7.5 Hz, 1H), 6.96 (dd, J = 8.7, 4.6 Hz, 2H), 6.45 (d, J = 7.4 Hz, 1H); ^{13}C NMR (75 MHz, acetone-D_6) δ 167.81, 151.27, 149.87, 149.37, 146.93, 144.29, 138.75,

*This paper was presented at the 12th International Conference on Atomically Controlled Surfaces, Interfaces and Nanostructures (ACSIN-12) in conjunction with the 21st International Colloquium on Scanning Probe Microscopy (ICSPM21), Tsukuba International Congress Center, Tsukuba, Japan, November 4-8, 2013.

†Corresponding author: rukkiat_j@hotmail.com

138.55, 131.79, 131.71, 130.32, 128.45, 126.99, 124.90, 123.43, 122.56, 119.81; Ms (ES^+): m/z(%) 681.1630 (M^+-PF_6, 100). The characterizations are also reported elsewhere [13–15].

(2) {(4-Methyl-1,10-phenanthroline-N-N')-bis-(2-phenylpyridine-$C^{2'}$,N)-iridium(III)}hexafluorophosphate: (0.08 g, 49%), ^{1}H NMR (300 MHz, acetone-D_6) δ 8.86 (d, J = 8.2 Hz, 1H), 8.50 (d, J = 9.1 Hz, 1H), 8.40 (t, J = 7.4 Hz, 2H), 8.23 (dd, J = 13.2, 6.7 Hz, 3H), 8.01 (dd, J = 8.2, 5.1 Hz, 1H), 7.88 (dd, J = 14.3, 7.1 Hz, 5H), 7.66 (d, J = 5.6 Hz, 2H), 6.99 (ddd, J = 18.5, 14.8, 7.3 Hz, 6H), 6.54-6.36 (m, 2H), 2.99 (s, 3H); ^{13}C NMR (75 MHz, $CDCl_3$) δ 205.44, 167.84, 167.80, 151.25, 150.44, 150.27, 149.27, 149.23, 147.03, 146.50, 144.35, 144.28, 138.64, 138.52, 131.84, 131.79, 131.46, 131.30, 130.29, 128.09, 127.52, 126.85, 125.09, 124.89, 123.46, 123.44, 122.47, 119.80, 18.22; Ms (ES^+): m/z(%) 740.1618 (M^+-PF_6+2Na^+, 100).

(3) {(2,9-Dimethyl-1,10-phenanthroline-N-N')-bis-(2-phenylpyridine-$C^{2'}$,N)-iridium(III)}hexafluorophosphate: (0.145 g, 91%), ^{1}H NMR (300 MHz, $CDCl_3$) δ 8.72 (d, J = 8.3 Hz, 1H), 8.23 (t, J = 3.7 Hz, 2H), 7.92 (t, J = 7.8 Hz, 1H), 7.82 (t, J = 6.9 Hz, 3H), 7.01 (t, J = 6.6 Hz, 1H), 6.95 (t, J = 7.6 Hz, 1H), 6.79 (t, J = 7.4 Hz, 1H), 6.21 (d, J = 7.6 Hz, 1H), 2.21 (s, 3H); ^{13}C NMR (75 MHz, Acetone-D_6) δ 205.34, 205.07, 167.85, 165.19, 150.15, 148.95, 148.00, 143.48, 139.22, 138.50, 131.57, 130.04, 129.71, 128.03, 127.24, 124.82, 123.04, 122.10, 119.80, 26.8; Ms (ES^+): m/z(%) 709.1943 (M^+-PF_6, 100). The characterizations are also reported elsewhere [16].

(4) {(4,7-Dimethyl-1,10-phenanthroline-N-N')-bis-(2-phenylpyridine-$C^{2'}$,N)-iridium(III)}hexafluorophosphate: (0.15 g, 94%), ^{1}H NMR (300 MHz, $CDCl_3$) δ 8.24 (s, 1H), 8.08 (d, J = 5.1 Hz, 1H), 7.87 (d, J = 8.1 Hz, 1H), 7.74-7.58 (m, 2H), 7.52 (d, J = 5.1 Hz, 1H), 7.34 (d, J = 5.5 Hz, 1H), 7.04-6.79 (m, 3H), 6.39 (d, J = 7.3 Hz, 1H), 2.85 (s, 3H); ^{13}C NMR (75 MHz, $CDCl_3$) δ 167.72, 150.33, 150.16, 148.94, 148.56, 146.45, 143.85, 138.16, 131.93, 131.03, 130.62, 127.23, 124.73, 123.40, 122.53, 119.58, 19.04; Ms (ES^+): m/z(%) 709.1943 (M^+-PF_6, 100). The characterizations are also reported elsewhere [17].

(5) {(3,4,7,8-Tetramethyl-1,10-phenanthroline-N-N')-bis-(2-phenylpyridine-$C^{2'}$,N)-iridium(III)} hexafluorophosphate: (0.15 g, 92%); ^{1}H NMR (300 MHz, $CDCl_3$) δ 8.26 (s, 1H), 7.91 (s, 1H), 7.89 (d, J = 8.3 Hz, 1H), 7.68 (t, J = 6.9 Hz, 2H), 7.36 (d, J = 5.6 Hz, 1H), 7.02 (t, J = 7.1 Hz, 1H), 6.92 (dd, J = 10.6, 6.1 Hz, 2H), 6.38 (d, J = 7.3 Hz, 1H), 2.78 (s, 3H), 2.36 (s, 3H); ^{13}C NMR (75 MHz, $CDCl_3$) δ 167.80, 151.03, 150.60, 148.70, 146.38, 145.41, 143.74, 137.88, 135.06, 131.88, 130.67, 130.02, 124.63, 124.42, 123.31, 122.42, 119.41, 18.07, 14.99; Ms (ES^+): m/z(%) 737.2256 (M^+-PF_6, 100). The characterizations are also reported elsewhere [15].

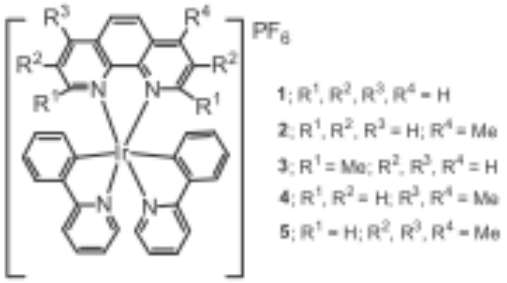

FIG. 1: The molecular structure of complex **1-5**.

The electroluminescence was fabricated with a solution of the iridium complexes in acetonitrile with a concentration of 12.5 mg ml^{-1}. Prior to the fabrication, the ITO glass substrates were thoroughly cleaned, followed by UV-ozone treatment. A thin film of PEDOT:PSS layer was spin coated at 3000 rpm for 180 s and baked at 260°C for 10 min. For simple LEC device, the complex **1-5** film was spin-coated with poly(9-vinylcarbazole) (PVK) as a host at 1:4 mole ratio, followed by the aluminum cathode using a shadow mask under high vacuum. For the OLED device, 1,3,5-tris(2-N-phenylbenzimidazolyl)benzene (TPBI) and LiF were used before aluminum cathode. The electroluminescent properties of the resultant devices were performed using Keithley characterization systems. The current density and luminance versus voltage sweeps were measured using a Keithley 2400 source meter and calibrated with a silicon photodiode.

III. RESULTS AND DISCUSSION

The molecular structure of complex **1-5** is depicted in Fig. 1. The charged iridium(III) complexes were designed with 2-phenyl pyridine as the C,N ligand and 1,10-phenanthroline as the N,N' ligand by varying the number and the position of methyl groups.

The solution absorption and emission of complex **1-5** were shown in Fig. 2. The strong absorption bands below 300 nm can be assigned as the spin-allowed π–π^* transition in the ligand-centered (LC) transition of the cyclometalated phenyl pyridine (pqy) and phenanthroline (phen) while the weak absorption region shows at 385-500 nm corresponding to metal-to-ligand charge transfer (MLCT) transition, respectively. These characteristic are consistent with the previously reported of the literature data [14–17]. The emission wavelength of the complex **1-5** shows at 518-547 nm with the emission quantum yield about 0.01-0.02 using a solution of quinine sulfate served as the standard. We found that the photo physic properties of the solution and thin film data are slightly red shifted. These characteristic indicated that the aggregate was formed in solid thin film. The photophysic data are summarized in Table I.

TABLE I: Photophysical characteristics of solution and thin film from complex **1-5**.

Complex	DCM solution			Thin film[a]	
	λ_{abs} (nm, log ε)	λ_{em} (nm)	Φ_{PL}	λ_{abs} (nm)	λ_{em} (nm)
1	267 (4.9), 381 (4.0), 418 (3.7)	547	0.01	385, 421	551
2	267 (4.7), 381 (3.7), 414 (3.4)	540	0.01	381, 424	545
3	271 (4.3), 375 (3.2), 419 (2.7)	524	0.02	420	536
4	268 (4.7), 381 (3.8), 416 (3.5)	535	0.01	418	540
5	272 (4.5), 343 (3.8), 421 (3.2)	518	0.01	424	538

[a]Spin-coated from DCM solution.

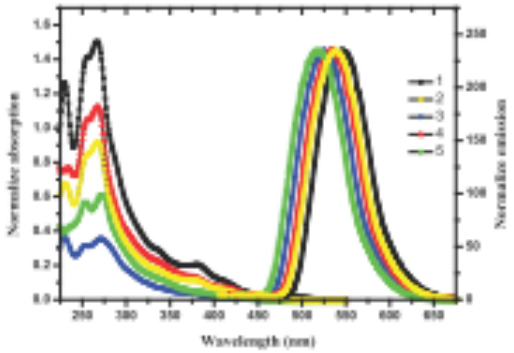

FIG. 2: The UV-Visible absorption and emission of complex **1-5**.

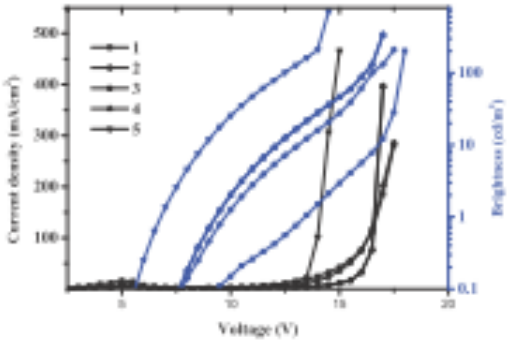

FIG. 3: Current density and brightness versus applied bias voltage of the device structure ITO/PEDOT:PSS /PVK: **1-5** (4:1)/Al.

The electroluminescences of the complex **1-5** were investigated with a simple LECs by using 4:1 host-guest ratio as in our previous study [18]. We fabricated the LEC device with the structure: ITO/PEDOT:PSS/PVK: **1-5** (4:1)/Al which PEDOT:PSS were used as a hole-injecting layer and PVK as the high triplet energy host polymer. We found that our host-guest LECs of complex **1** give significantly increase a brightness to 201 cdm^{-2} compared with a pure LECs device at 40 cdm^{-2} [14]. The results show that a maximum current efficiency at 1.35 cdA^{-1} at

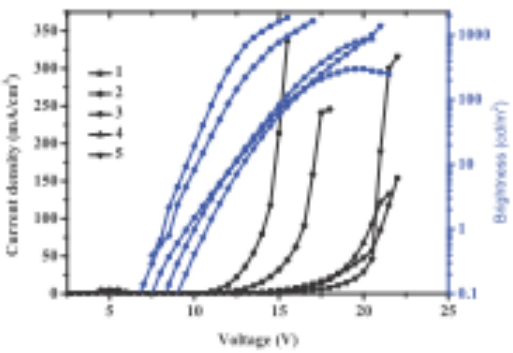

FIG. 4: Current density and brightness versus applied bias voltage of the device structure ITO/PEDOT:PSS /PVK: **1-5** (4:1)/TPBI/LiF/Al.

TABLE II: Host-guest LEC and OLED device performances of complex **1-5**.

complex	$V_{turn-on}$ (V)	L_{max} (cdm^{-2})	η_c (cdA^{-1})	η_p (lmW^{-1})	CIE (x, y)
1[a]	13.4	201	0.13	0.02	0.46, 0.63
2[a]	9.8	289	0.14	0.04	0.41, 0.53
3[a]	9.3	337	0.55	0.14	0.39, 0.58
4[a]	9.3	393	0.55	0.14	0.40, 0.59
5[a]	6.8	717	1.35	0.42	0.31, 0.55
1[b]	13.4	299	1.67	0.38	0.33, 0.49
2[b]	9.8	1,642	3.49	0.89	0.30, 0.50
3[b]	9.3	1,200	4.49	1.14	0.30, 0.54
4[b]	9.3	1,859	2.90	0.83	0.26, 0.47
5[b]	6.8	1,376	4.28	0.84	0.30, 0.52

[a]Device 1: ITO/PEDOT:PSS/PVK: **1-5** (4:1)/Al
[b]Device 2: ITO/PEDOT:PSS/PVK: **1-5** (4:1)/TPBI/LiF/Al

the brightness 710 cdm^{-2} can be observed with complex **5** (Fig. 3).

To further study the host-guest EL properties, the complex **1-5** were fabricated with OLED structure: ITO/PEDOT:PSS/PVK: **1-5** (4:1)/TPBI/LiF/Al. The device inserted TBBI/LiF as the electron transporting layers. All OLEDs gave more efficient electroluminescence than simple LEC devices which can be explained by the energy profile [9, 19]. The best device can be achieved from complex **3** with a current efficiency of 4.49 cdA^{-1}, maximum brightness at 1,200 cdm^{-2}, turn on voltage of 9.3 V and CIE coordinates at 0.30, 0.54 (Fig. 4). All the

electrical characteristics are summarized in Table II.

IV. CONCLUSIONS

The series of charged Ir(III) complexes with 1,10-phenanthroline as N,N ligand have been synthesized and fabricated with host-guest electroluminescence. Our devices demonstrated that OLEDs give a better efficient than LECs device. The results show that ITO/PEDOT:PSS/PVK: **3** (4:1)/TPBI/LiF/Al give a maximum current efficiency at 4.49 cdA^{-1} and maximum brightness at 1,200 cdm^{-2}.

Acknowledgments

This work was financially supported by the Thailand Research Fund, the Higher Education Commission and Ubon Ratchathani University (MRG5480005). Usana Mahanitipong thanks to the Young Scientist and Technologist Program (YSTP) for the scholarship.

[1] J. Slinker, D. Bernards, P. L. Houston, H. D. Abruna, S. Bernhard, and G. G. Malliaras, Chem. Commun. **19**, 2392 (2003).
[2] J. D. Slinker, J. Rivnay, J. S. Moskowitz, J. B. Parker, S. Bernhard, H. D. Abruna, and G. G. Malliaras, J. Mater. Chem. **17**, 2976 (2007).
[3] R. C. Evans, P. Douglas, and C. J. Winscom, Coord. Chem. Rev. **250**, 2093 (2006).
[4] G.-G. Shan, D.-X. Zhu, H.-B. Li, P. Li, Z.-M. Su, and Y. Liao, Dalton Trans. **40**, 2947 (2011).
[5] L. He, L. Duan, J. Qiao, G. Dong, L. Wang, and Y. Qiu, Chem. Mater. **22**, 3535 (2010).
[6] H.-B. Wu, H.-F. Chen, C.-T. Liao, H.-C. Su, and K.-T. Wong, Org. Electron. **13**, 483 (2012).
[7] H. A. Al-Attar, G. C. Griffiths, T. N. Moore, M. Tavasli, M. A. Fox, M. R. Bryce, and A. P. Monkman, Adv. Funct. Mater. **21**, 2376 (2011).
[8] R. D. Costa, O. Enrique, H. J. Bolink, S. Graber, C. E. Housecroft, and E. C. Constable, Adv. Funct. Mater. **20**, 1511 (2010).
[9] L. He, L. Duan, J. Qiao, D. Zhang, G. Dong, L. Wang, and Y. Qiu, Synth. Met. **160**, 52 (2013).
[10] C. D. Sunesh, M. Chandiran, G. Mathai, and Y. Choe, Opt. Mater. **35**, 407 (2013).
[11] T. Hu, L. Duan, J. Qiao, L. He, D. Zhang, L. Wang, and Y. Qiu, Synth. Met. **163**, 33 (2013).
[12] L. He, J. Qiao, L. Duan, G. Dong, D. Zhang, L. Wang, and Y. Qiu, Adv. Funct. Mater. **19**, 2950 (2009).
[13] C. Rothe, C.-J. Chiang, V. Jankus, K. Abdullah, X. Zeng, R. Jitchati, A. S. Batsanov, M. R. Bryce, and A. P. Monkman, Adv. Funct. Mater. **19**, 2038 (2009).
[14] R. D. Costa, E. Ortí, H. J. Bolink, S. Graber, S. Schaffner, M. Neuburger, C. E. Housecroft, and E. C. Constable, Adv. Funct. Mater. **19**, 3456 (2009).
[15] M. S. Lowry, W. R. Hudson, R. A. Pascal, and S. Bernhard, J. Am. Chem. Soc. **126**, 14129 (2004).
[16] D. B. Moon and Y. S. Choe, Mol. Cryst. Liq. Cryst. **584**, 60 (2013).
[17] C. Dragonetti, L. Falciola, P. Mussini, S. Righetto, D. Roberto, R. Ugo, A. Valore, F. DeAngelis, S. Fantacci, A. Sgamellotti, M. Ramon, and M. Muccini, Inorg. Chem. **46**, 8533 (2007).
[18] P. Khamtoem, S. Sahasithiwat, M. A. Fox and R. Jitchati, e-J. Surf. Sci. Nanotech. (Submitted).
[19] F. Dumur, D. Bertin, C. R. Mayer, A. Guerlin, G. Wantz, G. Nasr, E. Dumas, F. Miomandre, G. Clavier, and D. Gigmes, Synth. Met. **161**, 1934 (2011).

EurJIC European Journal of Inorganic Chemistry
ChemPubSoc Europe
FULL PAPER

DOI:10.1002/ejic.201400007

Intramolecular π Stacking in Cationic Iridium(III) Complexes with Phenyl-Functionalized Cyclometalated Ligands: Synthesis, Structure, Photophysical Properties, and Theoretical Studies

Peng Li,[a,b] Guo-Gang Shan,[b] Hong-Tao Cao,[b] Dong-Xia Zhu,*[b] Zhong-Min Su,*[a,b] Rukkiat Jitchati,[c,d] and Martin R. Bryce*[c]

Keywords: Iridium / Luminescence / Photophysics / Density functional calculations / Light-emitting cells

The syntheses of two new heteroleptic cationic iridium complexes containing 2,6-diphenylpyridine (Hdppy) and 2,4,6-triphenylpyridine (Htppy) as the cyclometalated ligands, namely, $[Ir(dppy)_2phen]PF_6$ (**1**, phen = 1,10-phenanthroline) and $[Ir(tppy)_2phen]PF_6$ (**2**), are described. The X-ray crystal structure of **2** reveals a distorted octahedral geometry around the Ir center and close intramolecular face-to-face π–π stacking interactions between the pendant phenyl rings at the 2-position of the cyclometalated ligands and the N^N ancillary ligand. This represents a new π–π stacking mode in charged Ir complexes. Complexes **1** and **2** are green photoemitters: their photophysical and electrochemical properties are interpreted with the assistance of density functional theory (DFT) calculations. These calculations also establish that the observed intramolecular interactions cannot effectively prevent the lengthening of the Ir–N bonds of the complexes in their metal-centered (^{3}MC) states. Complexes **1** and **2** do not emit light in light-emitting electrochemical cells (LECs) under conditions in which the model compound $[Ir(ppy)_2phen]PF_6$ (**3**) emits strongly. This is explained by degradation reactions of the ^{3}MC state of **1** and **2** under the applied bias during LEC operation facilitated by the enhanced distortions in the geometry of the complexes. These observations have important implications for the future design of complexes for LEC applications.

Introduction

Cyclometalated Ir^{III} complexes have attracted considerable attention during the last decade owing to their synthetic versatility, high thermal stability, relatively short excited-state lifetimes, high photoluminescence efficiency, and good emission wavelength tunability.[1] They have been widely exploited as emitters in phosphorescent organic light-emitting diodes (PhOLEDs),[2,3] solid-state lighting,[4] and light-emitting electrochemical cells (LECs).[5] LECs offer advantages over conventional OLEDs owing to their simpler device architecture, the use of spin-coating techniques in their fabrication, and the use of air-stable electrodes without the need for rigorous encapsulation, all of which are applicable to large-area emission and cheap processing. In LECs, ionic transition metal complexes (iTMCs) of the generic formula $[(C^N)_2Ir(N^N)][PF_6]$ perform all the roles needed to generate light.[6] When an electrical bias is applied to the LEC, the iTMCs serve to (1) decrease the injection barriers through the displacement of the counterion, (2) transport the electrons and holes through consecutive reduction and oxidation processes, and (3) generate the photons. The devices can operate at very low voltages and yield high brightness and power efficiency with tunable emission color.

The practical applications of iTMC-based LECs are hampered by the current limitations of their stability.[7] Nucleophile-assisted ligand-exchange reactions at the metal center can occur, and the new complex that is formed can quench the luminescence. A strategy initiated by Bolink, Constable et al., which involves shielding the Ir atom of the iTMC by intramolecular π–π stacking (to form "an intramolecular cage"),[6a] has led to dramatic improvements in stability and enhanced lifetimes of the LECs.[8] For this purpose, phenyl groups have been attached at the α positions to the nitrogen atoms of the N^N ancillary ligands. For example, pendant phenyl group(s) on 2,2′-bipyridine (bpy),

[a] College of Chemistry, Jilin University, Qianjin Road 2699, Changchun 130023, P. R. China
[b] Institute of Functional Material Chemistry, Faculty of Chemistry, Northeast Normal University, Renmin Road 5268, Changchun 130024, P. R. China
E-mail: zhudx047@nenu.edu.cn
zmsu@nenu.edu.cn
http://en.nenu.edu.cn
[c] Department of Chemistry, Durham University, Durham DH1 3LE, U.K.
E-mail: m.r.bryce@durham.ac.uk
http://www.dur.ac.uk
[d] Chemistry Department, Ubon Ratchathani University, Warinchumrap, Ubon Ratchathani 34190, Thailand
Supporting information for this article is available on the WWW under http://dx.doi.org/10.1002/ejic.201400007.

© 2014 Wiley-VCH Verlag GmbH & Co. KGaA, Weinheim

1,1-phenanthroline (phen), and 2-(1*H*-pyrazol-1-yl)pyridine (pzpy) ligands engage in face-to-face intramolecular π–π stacking interactions with the cyclometalating C^N ligands.[8,9] These interligand interactions effectively close the complexes in the ground states (S_0), the emitting (T_1) states, and the metal-centered (^{3}MC) triplet excited states and, thereby, protect the complexes from attack by nucleophiles such as water.[8b]

Similarly, our group has reported cationic Ir^{III} complexes based on the 2-(5-phenyl-2-phenyl-2*H*-1,2,4-triazol-3-yl)-pyridine (Phtz) ancillary ligand, which also show intramolecular π–π interactions. Density functional theory (DFT) calculations clearly indicated that these interactions reduce the possibility of ligand-exchange degradation reactions.[10] We note that Duan et al. reported that phenyl substitution of the N-heterocyclic carbene ancillary ligand of $[Ir(ppy)_2(pyphmi)]PF_6$ [Hppy = 2-phenylpyridine, pyphmi = 3-phenyl-1-(2-pyridyl)imidazolin-2-ylidene-C,$C^{2'}$] leads to weak π–π interactions and increased torsion angles, which do not enhance the stability of the LECs.[5g]

To the best of our knowledge, the π-stacking strategy has exclusively involved pendant phenyl substitution of the ancillary ligand.[8–11] The aim of the present work is to address a fundamental question: what is the effect of attaching pendant phenyl substituents to the cyclometalating (C^N) ligands? We now present the synthesis and characterization of two new complexes $[Ir(dppy)_2(phen)][PF_6]$ (**1**) and $[Ir(tppy)_2(phen)][PF_6]$ (**2**) (Hdppy = 2,6-diphenylpyridine, Htppy = 2,4,6-triphenylpyridine) (Figure 1). An X-ray crystal structure analysis of **2** shows strong intramolecular π–π stacking interactions. The photophysical and electrochemical properties of **1** and **2** are reported, along with DFT/time-dependent DFT (TD-DFT) calculations. LECs have been fabricated from **1** and **2**, and the data are compared with those of the archetypal parent complex $[Ir(ppy)_2(phen)][PF_6]$ (**3**), which serves as a reference.

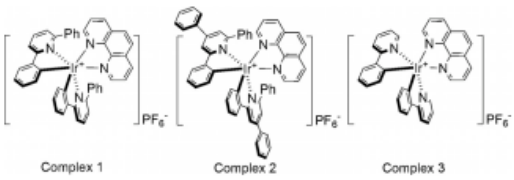

Figure 1. Chemical structures of **1** and **2** and the parent complex **3**, which is included for comparison.

Results and Discussion

Synthesis

The synthesis of **1** and **2** (Figure 1) followed the standard routes for complexes of the generic formula $[(C^N)_2Ir(N^N)][PF_6]$. The low yield for the formation of **1** and **2** is due to the steric hindrance from the *o*-phenyl substituents, as observed previously with sterically hindered C^N ligands.[12] The complexes were unambiguously characterized by ^{1}H NMR spectroscopy, mass spectrometry, and elemental analysis.

X-ray Crystal Structure of 2

The solid-state structure of **2** was determined by single-crystal X-ray diffraction. As depicted in Figure 2, complex **2** adopts a distorted octahedral geometry around the Ir center.

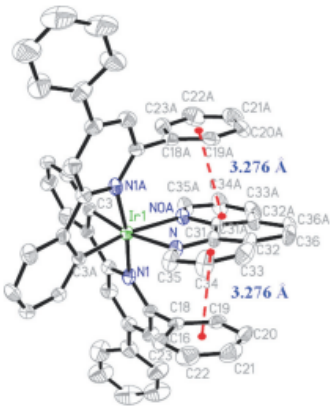

Figure 2. The X-ray molecular structure of the cation in **2**; the centroid-to-centroid distances are included.

The structure is characterized by the small C(3)–Ir(1)–N(1) (80.48°), C(3A)–Ir(1)–N(1) (80.48°), and N–Ir(1)–N(OA) (75.57°) bite angles and twisted C(3)–Ir(1)–N (169.59°), C(3A)–Ir(1)–N(OA) (169.59°), and N–Ir(1)–N(OA) (172.19°) bond angles. The Ir–N(phen) (2.209 Å), Ir–C(tppy) (2.005 Å), and Ir–N(tppy) (2.074 Å) distances of **2** closely resemble those previously reported for the parent complex **3**: Ir–N(phen) 2.137 and 2.150 Å, Ir–C(ppy) 2.003 and 2.017 Å, Ir–N(ppy) 2.043 and 2.048 Å.[8c] However, there are small differences in some of the bond lengths between structures **2** and **3** as a consequence of the steric interactions of the pendent phenyl groups in **2**. Specifically, the Ir–N(tppy) (ca. 2.074 Å) and Ir–N(phen) (ca. 2.209 Å) bonds of **2** are slightly longer than the comparable bonds in **3** [Ir–N(ppy) ca. 2.05 Å, Ir–N(phen) ca. 2.14 Å].[8c] Figure 2 illustrates the double face-to-face π-stacking between the pendant phenyl ring of both tppy ligands and the ancillary phen ligand of **2**; the interaction is in an optimal offset arrangement at a separation (centroid-to–centroid) of 3.276 Å. This stacking distance is similar to those observed in the $[Ir(ppy)_2(pbpy)]^+$ and $[Ir(ppy)_2(dpbpy)]^+$ cations (pbpy and dpbpy are 6-phenyl-2,2′-bipyridine and 6,6′-diphenyl-2,2′-bipyridine, respectively).[8b] This observation confirms that an intramolecular caged structure is formed by introducing a pendant phenyl group at C(2) of the cyclometalating ppy unit.

 © 2014 Wiley-VCH Verlag GmbH & Co. KGaA, Weinheim

Table 1. Photophysical and electrochemical data for **1** and **2**.

	PL at room temperature						PL at 77 K[a]	Electrochemical data[a]	
	λ_{em}[a] [nm]	Φ_{PL}[b] (τ, μs)[a]	k_r[a,c] [×10^5]	k_{nr}[a,c] [×10^6]	λ_{em}[d] [nm]	Φ_{film}[d]	λ_{em} [nm]	E_{ox} [V]	E_{red} [V]
1	552	0.15 (0.23)	6.6	3.71	595	0.06	515, 552 (sh)	0.80	–1.58
2	546	0.06 (0.31)	2.0	3.06	552	0.10	517, 545 (sh)	0.80	–1.59
3	583	0.39 (0.23)	17.3	2.71	591	0.11	532	0.79	–1.58

[a] Data obtained in acetonitrile solution; λ_{exc} = 355 nm. [b] Estimated error of ±10%. [c] $k_r = \Phi_{PL} \times \tau^{-1}$. [d] Data obtained from a neat thin film.

Photophysical Properties

The absorption and emission spectra of **1** and **2** (Figure 3) at room temperature were recorded in degassed acetonitrile solutions. The photophysical characteristics are reported in Table 1. The strong absorption bands in the range 200–350 nm are assigned to spin-allowed π–π* transitions from the ligands. The relatively weak absorption bands that occur in the lower-energy region (350–500 nm) correspond to ^{1}MLCT (metal-to-ligand charge-transfer), ^{3}MLCT, ^{1}LLCT (ligand-to-ligand charge-transfer), ^{3}LLCT, and ligand-centered (LC) ^{3}π–π* transitions with reference to those reported for other Ir^{III} complexes.[13] This observation implies that the spin-forbidden ^{3}MLCT, ^{3}LLCT, and LC ^{3}π–π* transitions have gained considerable intensity by mixing with the higher-lying spin-allowed ^{1}MLCT transitions because of the strong spin–orbit coupling endowed by the iridium atom. Generally, for cationic Ir^{III} complexes, three excited states, namely, ^{3}MLCT, ^{3}LLCT, and LC ^{3}π–π*, contribute to light emission.[14] At room temperature, **1** and **2** exhibit intense green emission with peak values at 546 and 552 nm, respectively, in CH_3CN solutions. The broad and featureless bands indicate that the emissive excited states of these two complexes are predominantly ^{3}MLCT or ^{3}LLCT in character, rather than LC ^{3}π–π* transitions, which typically show vibronic structure in the emission spectra.[15] The emission spectra of **1** and **2** in CH_3CN solutions at 77 K remain broad and are blueshifted, which indicates that their excited states retain ^{3}MLCT and ^{3}LLCT character at low temperature.[14]

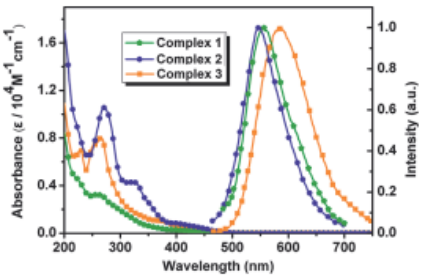

Figure 3. Absorption and normalized emission spectra of **1**, **2**, and **3** in CH_3CN solutions at room temperature.

As shown in Figure 3, the 2-phenyl substituents cause a significant blueshift in the emission wavelengths of **1** and **2** (31 and 37 nm, respectively) compared to that of **3**. The larger blueshift for **2** is ascribed to the additional electron-donating phenyl group at C(4) of the pyridyl ring.[16] The emission for **3** (λ_{max} = 583 nm in MeCN; Figure 3) is consistent with previously reported data for this complex (579 nm in MeCN;[17] 575 nm in CH_2Cl_2).[18] The emission spectra for **1**–**3** have the same trend in a non-coordinating solvent such as CH_2Cl_2 (see Figure S5 in the Supporting Information).

For **1** and **2** in CH_3CN, the photoluminescence quantum yields (PLQYs) are 0.15 and 0.06, respectively. Complex **1** shows a significantly higher radiative rate constant than that of **2**; this may be the reason that **1** has a higher PLQY in solution, as the nonradiative rate constants for both **1** and **2** are quite similar. Conversely, in thin films, the PLQY of **2** (Φ = 0.10) is higher than that for **1** (Φ = 0.06), as the steric bulk of the extra phenyl substituent now has the beneficial effect of reducing self-quenching. The excited-state lifetimes of **1** and **2** in solution are 0.23 and 0.31 μs, respectively, which are typical for phosphorescent emission in [(C^N)$_2$Ir(N^N)][PF$_6$] complexes.[8] The radiative decay rates (k_r) of **1**–**3** in CH_3CN solution were calculated as 6.6×10^5 for **1**, 2.0×10^5 for **2**, and 17.3×10^5 for **3**.

Electrochemical Properties

The electrochemical behavior of **1** and **2** in CH_3CN solution was investigated by cyclic voltammetry, and the data are reported versus ferrocene/ferrocenium in Table 1. Complexes **1** and **2** exhibit quasireversible oxidation and reduction peaks at E_{ox} = 0.80 V and E_{red} = –1.58/–1.59 V, respectively, which are very similar to the data obtained under the same conditions for **3** [0.79 and –1.58 V this work (cf. 0.85 and –1.54 V in CH_2Cl_2)].[19] These data are consistent with oxidation primarily at the Ir center and the phenyl ring of the cyclometalated ligand, whereas the reduction is localized on the ancillary ligand.

Quantum Chemical Calculations

The geometries and electronic structures of **1** and **2** were calculated by DFT/TD-DFT methods at the B3LYP/(6-31G*+LANL2DZ) level to provide additional insights into the structures and nature of the emissive excited states. Figure 4 displays the atomic orbital compositions of the lowest unoccupied and highest occupied molecular orbitals (LUMO and HOMO, respectively) of the cations of **1** and **2**. The LUMO of both complexes is almost the same and resides on the phenanthroline group. The HOMO is composed of a mixture of π orbitals of the phenyl group at C(2)

 © 2014 Wiley-VCH Verlag GmbH & Co. KGaA, Weinheim

of the cyclometalated ligands and iridium d orbitals: the phenyl groups at C(4) or C(6) make no contribution to the HOMOs. These data are consistent with studies on analogous complexes.[8] To further understand the emission processes of **1** and **2**, TD-DFT methods were used to calculate the low-lying triplet states (T_1) at the optimized geometry of the ground state (S_0). The orbital diagrams show that the T_1 state for **1** mainly originates from HOMO→LUMO (74%), and the T_1 state for **2** mainly originates from HOMO→LUMO+1 (56%) and HOMO→LUMO+3 (20%) transitions (Figure S6). These data suggest that the lowest excited states are induced by ^{3}MLCT (iridium→ancillary ligand) with some ^{3}LLCT character (cyclometalated ligands→phen). In addition, the unpaired-electron spin density distribution calculated for **1** and **2** perfectly matches the topology of the HOMO→LUMO excitation in which the T_1 state originates and confirms the mixed ^{3}MLCT/^{3}LLCT character of the lowest triplet state (Figure S7).[8d] The photophysical properties and the calculated results illustrate that the emission of **1** and **2** mainly originates from the T_1 states and agree with the experimentally observed broad unstructured emission spectra of both complexes (Figure 3).

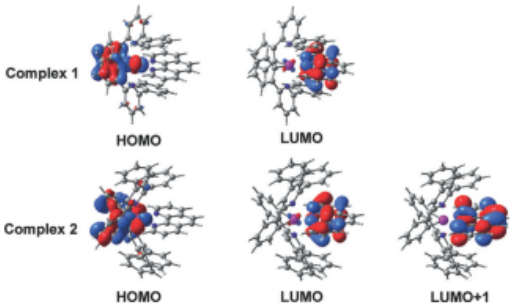

Figure 4. HOMO and LUMO distributions of **1** and **2**.

The metal-centered (^{3}MC) states result from the excitation of an electron from the occupied t_{2g} (dπ) HOMO to the unoccupied e_{2g} (dσ*) level, which is regarded as the origin of the degradation process for Ru^{II}- and Ir^{III}-based LECs.[7] In the ^{3}MC states, the rupture of metal–ligand bonds can induce opening of the structure and, thereby, enhance the reactivity of complex; thus, photodegradation is facilitated, and the device becomes unstable. The robust intramolecular π-stacking observed in the complexes reported by Bolink et al. minimizes the expansion of the metal–ligand bonds in the excited state, and this prevents the unwanted ligand-exchange reactions.[8] To evaluate the stability of **1** and **2**, the molecular structures of the ^{3}MC states were fully optimized from the minimum-energy structure of S_0 with Ir–N_{ppy} bond lengths lengthened to 2.70 Å.[8h] The metal-centered character of the triplet states for **1** and **2** was confirmed by the spin densities, which were calculated for the optimized ^{3}MC state geometries. The spin densities are mainly concentrated on the iridium atom with 1.47 eV unpaired electrons for both **1** and **2** in their ^{3}MC states. The key bond lengths that affect the stabilities of **1** and **2** in the ^{3}MC states are presented in Figure 5. The Ir–N_{phen} bond lengths of 2.23 Å for **1** and **2** in the ^{3}MC state are similar to the Ir–N_{phen} bond lengths (2.26 Å) in T_1. The structures show that the face-to-face π stacking, as observed in the X-ray crystal structure of **2** (Figure 2), is retained in the ^{3}MC states with centroid-to-centroid distances of 4.006 and 4.022 Å for **1** and **2**, respectively.

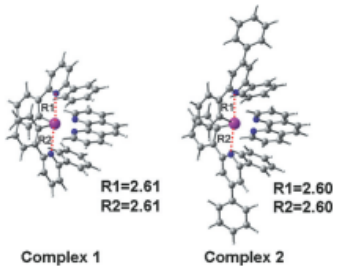

Figure 5. Minimum–energy structures calculated for the ^{3}MC states of **1** and **2**. Distances R1 and R2 are the optimized Ir–$N_{cyclometalated\ ligand}$ bond lengths [Å].

However, a crucial point is that the intramolecular π–π interactions in **1** and **2** do not prevent opening of the structure in the ^{3}MC state, unlike iridium complexes with a pendant phenyl group on the ancillary ligand such as $[Ir(ppy)_2(pbpy)]^+$.[8b] For example, as shown in Figure 5, the calculated Ir–N bond lengths (R1 and R2) of **1** increased from 2.13 Å in the ground state (S_0) to 2.61 Å in the ^{3}MC state, and the changes are the same in **2**. Complex **3** exhibits similar changes to the corresponding bond lengths (Figure S8).

Light-Emitting Cells (LECs)

To investigate the electroluminescent properties of the complexes, LECs were prepared with a structure of ITO/PEDOT:PSS (50 nm)/iridium complex–IL (molar ratio 4:1 w/w; 75 nm)/Al (120 nm). ITO is indium tin oxide, PEDOT:PSS is poly(3,4-ethylenedioxythiophene)/poly(styrene sulfonate), and IL is the ionic liquid 1-butyl-3-methylimidazolium hexafluorophosphate ($BMIMPF_6$), which reduces drastically the turn-on time of LECs and enhances the ionic conductivity of the thin film.[20] This is the standard LEC architecture that our groups have used previously.[21] As a benchmark, model complex **3** was studied in the present work. As expected, upon applying a bias of 3 V to the device with complex **3**, light emission was observed within a few minutes, as reported previously by us[19] and by Bolink et al.[8c] for this complex. However, for **1** and **2**, under identical conditions no light emission was observed even after the application of a bias of 3 V for as long as 24 h. Moreover, no light emission was observed at a higher bias (8 V) for 24 h. These studies demonstrate that

 © 2014 Wiley-VCH Verlag GmbH & Co. KGaA, Weinheim

although **1** and **2** show efficient photoluminescence they are not suitable for LECs. This can be explained by the distorted molecular structure induced by the double π stacking (as revealed by X-ray analysis) and by the theoretical calculations that show that the intramolecular π–π interactions in **1** and **2** do not effectively prevent the transition to a more open structure with an expanded Ir–N coordination sphere in the excited states. Consequently, we conclude that the double π stacking in **1** and **2** is detrimental to stability and it is likely that the complexes degrade in the excited state through reactions with adventitious nucleophiles and so luminescence is quenched.

Conclusions

This combined experimental and theoretical study has provided new insights into the established strategy of using intramolecular π–π stacking in cationic Ir^{III} complexes to enhance LEC performance. Complexes **1** and **2** possess the new feature of pendant phenyl rings at the α position to the nitrogen atom of the cyclometalating units. X-ray analysis of **2** shows that it has a distorted octahedral geometry with strong intramolecular face-to-face π–π stacking interactions between the pendant phenyl units and the ancillary ligands. DFT calculations establish that the intramolecular interactions are retained in the excited triplet states and that this mode of π–π stacking does not prevent the opening of the Ir–N coordination sphere in the excited states. Consequently, although the complexes are photoluminescent, they do not emit light in LECs under conditions in which the model compound $[Ir(ppy)_2phen]PF_6$, emits strongly. This is presumably because of degradation reactions of the ^3MC state of **1** and **2** under the applied bias during LEC operation. This combined experimental and theoretical study provides new insights into structure–property relationships in ionic Ir complexes and demonstrates convincingly that intramolecular π–π stacking can be detrimental to LEC performance in specific cases owing to enhanced distortions in the geometry of the complex. This is valuable information for the future design of complexes for LEC applications.

Experimental Section

Materials, Synthesis, and Characterization: All reagents and solvents employed were commercially available and used as received without further purification. The solvents for syntheses were freshly distilled from appropriate drying reagents. All experiments were performed under a nitrogen atmosphere by using standard Schlenk techniques. ^1H NMR spectra were measured with a Bruker Avance 500 MHz spectrometer with tetramethylsilane as the internal standard. Mass spectra were recorded by using matrix-assisted laser desorption-ionization time-of-flight (MALDI–TOF) mass spectrometry. Elemental analyses (C, H, and N) were obtained by using a Perkin–Elmer 240C elemental analyzer. UV/Vis absorption spectra were recorded with a Hitachi U3030 spectrometer. The emission spectra were recorded with a Hitachi F-7000 fluorescence spectrophotometer. The excited-state lifetimes were measured with a transient spectrofluorimeter (Edinburgh FLS920) with a time-correlated single-photon-counting technique. The photoluminescence quantum yields (PLQYs) in solution and in neat films were measured with an integrating sphere in a fluorospectrophotometer. Cyclic voltammetry was performed with a BAS 100 W instrument at a scan rate of 100 $mV\,s^{-1}$ in CH_3CN with a three-electrode configuration: a glassy-carbon electrode as the working electrode, an aqueous saturated calomel electrode as the pseudo-reference electrode, and a platinum wire as the counter electrode. A 0.1 M solution of tetra-*n*-butylammonium perchlorate (TBAP) in CH_3CN was used as the supporting electrolyte, and ferrocene was selected as the internal standard.

Synthesis: Ligands Hdppy[12] and Htppy[12] and complex **3**[17] were synthesized as described in the literature. The μ-dichloro-bridged diiridium C^N ligand complexes, which are precursors to complexes **1** and **2**, were synthesized from Hdppy and Htppy, respectively, by following standard literature procedures for analogs.[22]

$[Ir(dppy)_2(phen)][PF_6]$ (1): A mixture of 2,6-diphenylpyridine (508 mg, 2.2 mmol), $IrCl_3{\cdot}3H_2O$ (352 mg, 1.0 mmol), 2-ethoxyethanol (12 mL), and water (4 mL) was heated at 120 °C. After 12 h, the mixture was cooled to 20 °C, and the precipitate was collected by filtration, washed with water, and then dissolved in CH_2Cl_2. The organic solution was separated, dried with $MgSO_4$, filtered, and evaporated to give a pale green solid, presumed to be the bis-μ-chloro-bridged complex, which was used directly in the next step. A mixture of this complex (138 mg, 0.1 mmol) and phenanthroline (36 mg, 0.2 mmol) in dichloromethane (30 mL) and methanol (15 mL) was heated under reflux for 24 h in the dark. After cooling to room temperature, the mixture was filtered; an excess of solid KPF_6 was then added, and the mixture was stirred for 1 h at room temperature. The solvent was removed under reduced pressure, and the residue was purified by silica gel column chromatography with a mixture of dichloromethane/ethyl acetate (4:1 v/v) as eluent to yield **1** (8 mg) as a yellow solid. ^1H NMR (500 MHz, $CDCl_3$): δ = 8.20 (d, J = 7.5 Hz, 2 H), 8.02 (d, J = 7.5 Hz, 2 H), 7.98 (s, 2 H), 7.88 (d, J = 7.5 Hz, 2 H), 7.63–7.67 (m, 4 H), 7.20–7.24 (m, 6 H), 7.02 (t, J = 7.5 Hz, 2 H), 6.81 (d, J = 8 Hz, 2 H), 6.62 (t, J = 3.5 Hz, 4 H), 6.48 (d, J = 8 Hz, 2 H), 6.11 (s, 2 H), 5.01 (d, J = 7 Hz, 2 H) ppm. $C_{48}H_{36}F_6IrN_4P$ (1006.02): calcd. C 57.31, H 3.61, N 5.57; found C 57.36, H 3.65, N 5.61. ESI-MS: m/z = 833.2 $[M - PF_6]^+$.

$[Ir(tppy)_2(phen)][PF_6]$ (2): By following the same procedure as that for **1**, 2,4,6-triphenylpyridine (676 mg, 2.2 mmol) gave a pale green solid, presumed to be the bis-μ-chloro-bridged complex, which was used directly in the next step. A mixture of this complex (168 mg, 0.1 mmol) and phenanthroline (36 mg, 0.2 mmol) in dichloromethane (30 mL) and methanol (15 mL) was heated under reflux for 24 h in the dark. Workup and purification as described for **1** yielded **2** (15 mg). ^1H NMR (500 MHz, $[D_6]$dimethyl sulfoxide: δ = 8.69 (d, J = 1.5 Hz, 2 H), 8.37–8.42 (m, 4 H), 8.07 (s, 2 H), 7.98–8.00 (m, 4 H), 7.67 (d, J = 4 Hz, 2 H), 7.48–7.50 (m, 8 H), 7.17–7.22 (m, 4 H), 7.03–7.06 (m, 2 H), 6.96 (d, J = 2 Hz, 2 H), 6.84 (d, J = 7.5 Hz, 2 H), 6.64 (t, J = 7.5 Hz, 2 H), 6.56 (t, J = 7.5 Hz, 2 H), 6.06 (t, J = 7.5 Hz, 2 H), 5.11 (d, J = 7.5 Hz, 2 H) ppm. $C_{60}H_{44}F_6IrN_4P$ (1158.22): calcd. C 62.22, H 3.83, N 4.84; found C 62.27, H 3.91, N 4.88. ESI-MS: m/z = 983.2 $[M - PF_6]^+$. Single crystals of **2** were obtained by slow evaporation of a dilute CH_2Cl_2 solution of the complex.

X-ray Crystallography: The data collection for **2** was performed with a Bruker Smart Apex II CCD diffractometer with graphite-monochromated Mo-K_α radiation (λ = 0.71069 Å) at 293 K. Absorption corrections were performed by using the multiscan tech-

 © 2014 Wiley-VCH Verlag GmbH & Co. KGaA, Weinheim

nique. The crystal structure was solved by direct methods with SHELXTL-97[23] and refined by full-matrix least-squares techniques by using SHELXTL-97 within WINGX.[24] The hydrogen atoms of the aromatic rings were included in the structure factor calculation at idealized positions by using a riding model. Anisotropic thermal parameters were used to refine all non-hydrogen atoms except for some of the nitrogen and carbon atoms. Structural data in CIF format is available as Supporting Information. CCDC-956631 contains the supplementary crystallographic data for this paper. These data can be obtained free of charge from The Cambridge Crystallographic Data Centre via www.ccdc.cam.ac.uk/data_request/cif.

Theoretical Calculations: The ground and excited electronic states of the complexes were investigated by performing DFT and TD-DFT calculations at the B3LYP level.[25] The 6-31G* basis sets were employed to optimize the C, H, N atoms, and the LANL2DZ basis sets were employed for the Ir atom. An effective core potential (ECP) replaces the inner core electrons of iridium to leave the outer core $(5s)^2(5p)^6$ electrons and the $(5d)^6$ valence electrons of the Ir^{III} ion. The geometry of the metal-centered triplet (^{3}MC) was fully optimized and calculated at the spin-unrestricted UB3LYP level with a spin multiplicity of three. All calculations reported here were performed with the Gaussian 09 software package.[26]

Device Preparation and Characterization: PEDOT:PSS is poly(3,4-ethylenedioxythiophene):poly(styrene sulfonate) (CLEVIOS™ P VP Al 4083 aqueous dispersion, 1.3–1.7% solid content Heraeus); solvents were obtained from Aldrich. ITO-coated glass substrates (20 Ω/sq) were cleaned and treated with oxygen plasma before use. The PEDOT:PSS layer was spin-coated onto the ITO substrate and baked at 100 °C for 30 min to yield a film with a thickness of ca. 100 nm. After cooling to room temperature, the solutions of **1**–**3** and the ionic liquid 1-butyl-3-methylimidazolium hexafluorophosphate ($BMIMPF_6$) in CH_2Cl_2 were spin-coated onto the substrate, and then the layer with a thickness of ca 90 nm was baked at 80 °C for 2 h. The film was transferred into a metal evaporating chamber in which an aluminum cathode (120 nm) was evaporated under low pressure ($<5\times10^{-4}$ mbar). The electroluminescence (EL) spectra were obtained with a Photo Research PR650 spectrophotometer under ambient conditions by applying a constant voltage with a Keithley 2400 source meter.

Supporting Information (see footnote on the first page of this article): ^{1}H NMR spectra of **1** and **2**; cyclic voltammograms of **1**–**3**; theoretical calculations of **1**–**3**; emission spectra of **1**–**3** in solution.

Acknowledgments

The authors gratefully acknowledge financial support from the National Natural Science Foundation of China (NSFC) (grant numbers 51203017, 20971020, 20903020, 21273030, 21131001, and 21303012), the 973 Program (2009CB623605), the Science and Technology Development Planning of Jilin Province (grant numbers 20100540, 201101008, and 20130522167JH), and the Fundamental Research Funds for the Central Universities (grant number 12QNJJ012). R. J. thanks the Royal Thai Government for a scholarship (grant number MRG5480005).

[1] a) V. W.-W. Yam, K. M.-C. Wong, *Chem. Commun.* **2011**, *47*, 11579; b) J. D. Routledge, A. J. Hallett, J. A. Platts, P. N. Horton, S. J. Coles, S. J. A. Pope, *Eur. J. Inorg. Chem.* **2012**, 4065.
[2] H. Yersin (Ed.), *Highly Efficient OLEDs with Phosphorescent Materials*, Wiley-VCH, Weinheim, Germany, **2008**.
[3] K. Walzer, B. Maennig, M. Pfeiffer, K. Leo, *Chem. Rev.* **2007**, *107*, 1233.
[4] K. T. Kamtekar, A. P. Monkman, M. R. Bryce, *Adv. Mater.* **2010**, *22*, 572.
[5] a) Q. Pei, G. Yu, C. Zhang, Y. Yang, A. J. Heeger, *Science* **1995**, *269*, 1086; b) K. M. Maness, R. H. Terrill, T. J. Meyer, R. W. Murray, R. M. Wightman, *J. Am. Chem. Soc.* **1996**, *118*, 10609; c) J. K. Lee, D. S. Yoo, E. S. Handy, M. F. Rubner, *Appl. Phys. Lett.* **1996**, *69*, 1686; d) J. Slinker, D. Bernards, P. L. Houston, H. D. Abruna, S. Bernhard, G. G. Malliaras, *Chem. Commun.* **2003**, 2392; e) A. B. Tamayo, S. Garon, T. Sajoto, P. I. Djurovich, I. M. Tsyba, R. Bau, M. E. Thompson, *Inorg. Chem.* **2005**, *44*, 8723; f) F. De Angelis, S. Fantacci, N. Evans, C. Klein, S. M. Zakeeruddin, J.-E. Moser, K. Kalyanasundaram, H. J. Bolink, M. Grätzel, M. K. Nazeeruddin, *Inorg. Chem.* **2007**, *46*, 5989; g) F. L. Zhang, L. Duan, J. Qiao, G. F. Dong, L. D. Wang, Y. Qiu, *Org. Electron.* **2012**, *13*, 2442.
[6] Reviews: a) R. D. Costa, E. Ortí, H. J. Bolink, F. Monti, G. Accorsi, N. Armaroli, *Angew. Chem. Int. Ed.* **2012**, *51*, 8178; *Angew. Chem.* **2012**, *124*, 8300; b) T. Hu, L. Duan, Y. Qiu, *J. Mater. Chem.* **2012**, *22*, 4206; c) S. Ladouceur, E. Zysman-Colman, *Eur. J. Inorg. Chem.* **2013**, 2985.
[7] a) G. Kalyuzhny, M. Buda, J. McNeill, P. Barbara, A. J. Bard, *J. Am. Chem. Soc.* **2003**, *125*, 6272; b) J. D. Slinker, J.-S. Kim, S. Flores-Torres, J. H. Delcamp, H. D. Abruna, R. H. Friend, G. G. Malliaras, *J. Mater. Chem.* **2007**, *17*, 76; c) L. J. Soltzberg, J. Slinker, S. Flores-Torres, D. Bernards, G. G. Malliaras, H. D. Abruna, J. S. Kim, R. H. Friend, M. D. Kaplan, V. Goldberg, *J. Am. Chem. Soc.* **2006**, *128*, 7761.
[8] a) H. J. Bolink, E. Coronado, R. D. Costa, E. Ortí, M. Sessolo, S. Graber, K. Doyle, M. Neuburger, C. E. Housecroft, E. C. Constable, *Adv. Mater.* **2008**, *20*, 3910; b) R. D. Costa, E. Ortí, H. J. Bolink, S. Graber, C. E. Housecroft, M. Neuburger, S. Schaffner, E. C. Constable, *Chem. Commun.* **2009**, 2029; c) R. D. Costa, E. Ortí, H. J. Bolink, S. Graber, S. Schaffner, M. Neuburger, C. E. Housecroft, E. C. Constable, *Adv. Funct. Mater.* **2009**, *19*, 3456; d) R. D. Costa, E. Ortí, H. J. Bolink, S. Graber, C. E. Housecroft, E. C. Constable, *Adv. Funct. Mater.* **2010**, *20*, 1511; e) R. D. Costa, E. Ortí, H. J. Bolink, S. Graber, C. E. Housecroft, E. C. Constable, *J. Am. Chem. Soc.* **2010**, *132*, 5978; f) R. D. Costa, E. Ortí, H. J. Bolink, S. Graber, C. E. Housecroft, E. C. Constable, *Chem. Commun.* **2011**, *47*, 3207; g) A. M. Bünzli, H. J. Bolink, E. C. Constable, C. E. Housecroft, M. Neuburger, E. Ortí, A. Pertegás, J. A. Zampese, *Eur. J. Inorg. Chem.* **2012**, 3780; h) R. D. Costa, E. Ortí, D. Tordera, A. Pertegás, H. J. Bolink, S. Graber, C. E. Housecroft, L. Sachno, M. Neuburger, E. C. Constable, *Adv. Energy Mater.* **2011**, *1*, 282.
[9] L. He, L. Duan, J. Qiao, D. Zhang, L. Wang, Y. Qiu, *Chem. Commun.* **2011**, *47*, 6467.
[10] G.-G. Shan, H.-B. Li, D.-X. Zhu, Z.-M. Su, Y. Liao, *J. Mater. Chem.* **2012**, *22*, 12736.
[11] L. Sun, A. Galan, S. Ladouceur, J. D. Slinker, E. Zysman-Colman, *J. Mater. Chem.* **2011**, *21*, 18083.
[12] A. J. Wilkinson, H. Puschmann, J. A. K. Howard, C. E. Foster, J. A. G. Williams, *Inorg. Chem.* **2006**, *45*, 8685.
[13] a) S. Sprouse, K. A. King, P. J. Spellane, R. J. Watts, *J. Am. Chem. Soc.* **1984**, *106*, 6647; b) G. G. Shan, D. X. Zhu, H. B. Li, P. Li, Z. Su, Y. Liao, *Dalton Trans.* **2011**, *40*, 2947; c) L. He, J. Qiao, L. Duan, G. Dong, D. Zhang, L. Wang, Y. Qiu, *Adv. Funct. Mater.* **2009**, *19*, 2950.
[14] H. T. Cao, G. G. Shan, B. Zhang, P. Li, S. L. Sun, Z. M. Su, *J. Mol. Struct.* **2012**, 1029.
[15] a) N. Francesco, L. D. Massimo, C. Alessandra, B. Anna, P. Fausto, C. Sebastiano, *Organometallics* **2004**, *23*, 5856; b) G. G. Shan, H. B. Li, H. T. Cao, D. X. Zhu, P. Li, Z. M. Su, Y. Liao, *J. Organomet. Chem.* **2012**, *713*, 20.
[16] a) N. Tian, D. Lenkeit, S. Pelz, L. H. Fischer, D. Escudero, R. Schiewek, D. Klink, O. J. Schmitz, L. González, M. Schäferling, E. Holder, *Eur. J. Inorg. Chem.* **2010**, 4875; b) C. S. Chin,

 © 2014 Wiley-VCH Verlag GmbH & Co. KGaA, Weinheim

M. S. Eum, S. Y. Kim, C. Kim, S. K. Kang, *Eur. J. Inorg. Chem.* **2007**, 372; c) N. M. Shavaleev, F. Monti, R. D. Costa, R. Scopelliti, H. J. Bolink, E. Ortí, G. Accorsi, N. Armaroli, E. Baranoff, M. Grätzel, M. K. Nazeeruddin, *Inorg. Chem.* **2012**, *51*, 2263; d) J. Li, P. I. Djurovich, B. D. Alleyne, M. Yousufuddin, N. N. Ho, J. C. Thomas, J. C. Peters, R. Bau, M. E. Thompson, *Inorg. Chem.* **2005**, *44*, 1713.

[17] C. Dragonetty, L. Falciola, P. Mussini, S. Righetto, D. Roberto, R. Ugo, A. Valore, F. DeAngelis, S. Fantacci, A. Sgamellotti, M. Ramon, M. Muccini, *Inorg. Chem.* **2007**, *46*, 8533.

[18] J. I. Goldsmith, W. R. Hudson, M. S. Lowry, T. H. Anderson, S. Bernhard, *J. Am. Chem. Soc.* **2005**, *127*, 7502.

[19] C. Rothe, C.-J. Chiang, V. Jankus, K. Abdullah, X. Zeng, R. Jitchati, A. S. Batsanov, M. R. Bryce, A. P. Monkman, *Adv. Funct. Mater.* **2009**, *19*, 2038.

[20] S. T. Parker, J. Slinker, M. S. Lowry, M. P. Cox, S. Bernhard, G. G. Malliaras, *Chem. Mater.* **2005**, *17*, 3187.

[21] J. Zhang, L. Zhou, H. A. Al-Attar, K. Z. Shao, L. Wang, D. X. Zhu, Z. M. Su, M. R. Bryce, A. P. Monkman, *Adv. Funct. Mater.* **2013**, *23*, 4667.

[22] M. Nonoyama, *Bull. Chem. Soc. Jpn.* **1974**, *47*, 767.

[23] G. M. Sheldrick, *SHELXL-97, Program for Crystal Structure Refinement*, University of Gōttingen, Germany, **1997**.

[24] L. J. Farrugia, *WINGX, A Windows Program for Crystal Structure Analysis*, University of Glasgow, U.K., **1988**.

[25] a) C. Lee, W. Yang, R. G. Parr, *Phys. Rev. B* **1998**, *37*, 785; b) A. D. Becke, *J. Chem. Phys.* **1993**, *98*, 5648.

[26] M. J. Frisch, G. W. Trucks, H. B. Schlegel, G. E. Scuseria, M. A. Robb, J. R. Cheeseman, G. Scalmani, V. Barone, B. Mennucci, G. A. Petersson, H. Nakatsuji, M. Caricato, X. Li, H. P. Hratchian, A. F. Izmaylov, J. Bloino, G. Zheng, J. L. Sonnenberg, M. Hada, M. Ehara, K. Toyota, R. Fukuda, J. Hasegawa, M. Ishida, T. Nakajima, Y. Honda, O. Kitao, H. Nakai, T. Vreven, J. A. Montgomery Jr., J. E. Peralta, F. Ogliaro, M. Bearpark, J. J. Heyd, E. Brothers, K. N. Kudin, V. N. Staroverov, R. Kobayashi, J. Normand, K. Raghavachari, A. Rendell, J. C. Burant, S. S. Iyengar, J. Tomasi, M. Cossi, N. Rega, J. M. Millam, M. Klene, J. E. Knox, J. B. Cross, V. Bakken, C. Adamo, J. Jaramillo, R. Gomperts, R. E. Stratmann, O. Yazyev, A. J. Austin, R. Cammi, C. Pomelli, J. W. Ochterski, R. L. Martin, K. Morokuma, V. G. Zakrzewski, G. A. Voth, P. Salvador, J. J. Dannenberg, S. Dapprich, A. D. Daniels, Ö. Farkas, J. B. Foresman, J. V. Ortiz, J. Cioslowski, D. J. Fox, *Gaussian 09W*, revision A.02, Gaussian, Inc., Wallingford CT, **2009**.

Received: January 3, 2014
Published Online: April 3, 2014

 © 2014 Wiley-VCH Verlag GmbH & Co. KGaA, Weinheim

View publication stats

Vol. **127** (2015) *ACTA PHYSICA POLONICA A* No. 4

Proceedings of the 4th International Congress APMAS2014, April 24-27, 2014, Fethiye, Turkey

Highly Efficient Blue LECs Using Charged Iridium Complexes

K. Wongkhan[a], U. Mahanitipong[a], M. Srikaew[a], Y. Tantirunggrotchai[b], S. Sahasithiwat[c], R. Jitchati[a,*]

[a]Department of Chemistry, Faculty of Science,Ubon Ratchathani University, Ubon Ratchathani Province, 34190, Thailand

[b]National Metal and Materials Technology Center, 114 Thailand Science Park, Pahol-yothin Rd., Klong 1, Khlong Luang, Pathumthani 12120, Thailand

[c]Department of Chemistry, Faculty of Science and Technology, Thammasat University, Pathumthani, 12120 Thailand

Two heteroleptic charged iridium (III) species comprising two cyclometallating ligands and a neutral diimine ligand were synthesized and characterized, namely [(3,4,7,8-tetramethyl-1,10-phenanthroline-N-N')-bis-(2-(2,4-difluorophenyl)-5-(trifluoromethyl)pyridine-$C^{6'}$,N)-iridium (III)]hexafluorophosphate (UM01) and [(3,4,7,8-tetramethyl-1,10-phenanthroline-N-N')-bis-(2-(2',4'-difluoro-phenyl)-1*H*-pyrazole-$C^{6'}$,N)-iridium (III)]hexafluorophosphate (UM02). Both complexes were used as the blue emitter in OLED and LEC devices. We found that the optimized structure is ITO/PEDOT:PSS/complex:$BMIMPF_6$(1:1)/Al. The UM01 gave a current efficiency of 1.14 cd A^{-1}, whereas the UM02 shows a better CIE coordination at 0.19, 0.40.

DOI: 10.12693/APhysPolA.127.1109

PACS: 85.60.Bt; 85.60.Jb

1. Introduction

Heteroleptic charged iridium (III) species comprising two cyclometallating ligands and a neutral diimine ligand of generic formula $(C^N)_2Ir(N^N)^+$ have been of great interest as multifunctional chromophores for advanced optoelectronic applications [1–6]. The key properties of these complexes are their high stabilities, high luminescence quantum yields, short excited state lifetime and tunable emission energies. The photophysical properties of these phosphors can be tuned by varying the ligand or its substituent groups and by the use of additional ancillary ligands [7]. A charged Ir (III) complex is the key component in highly efficient organic light-emitting diodes (OLEDs) and simple device light-emitting electrochemical cells (LECs) [8]. OLEDs and LECs have been made and studied during recent years motivated by their potential for applications in display and lighting. Today, the devices that are still far from experiencing a successful market entrance and many issues have to be solved in order to make them a viable alternative to the current display technologies. One big problem that should be intensive studied is the development of the blue emitter materials [9, 10]. For example, a charged iridium (III) demonstrated by Henk J. Bolink give a blue-green from LECs with a current efficiency reaching 5.5 cd A^{-1} and a maximum power efficiency of 5.8 Lm $Watt^{-1}$ [9]. Yong Qiu shows that LECs based on the charged iridium (III) of (2,4-difluorophenyl)-1*H*-pyrazole and 2-(1-(4-tritylphenyl)-1*H*-imidazol-2-yl)pyridine give highly efficient blue-green electroluminescence with current efficiency, external quantum efficiency, and power efficiency of 18.3 cd A^{-1}, 7.6%, and 18.0 lm W^{-1}, respectively [11]. Here, we developed the electroluminescence based on OLEDs and LECs from a charged iridium (III) complexes.

2. Experimental

All the chemicals were purchased from Acros organic and used without further purification, unless otherwise noted. The UM01 and UM02 were synthesized according to the reference by varying the C,N ligands [12]. ^{1}H and ^{13}C NMR spectra were recorded on a Bruker Avance 300 spectrometer. Chemical shifts are quoted downfield from internal standard TMS. MS data were obtained using a Thermo Finnigan LTQFT instrument. Ultraviolet-visible (UV-vis) spectra were recorded with Perkin-Elmer UV Lambda 25. Photoluminescence spectrum and the fluorescence quantum yields (Φ_f) were identified by a Perkin-Elmer LS 50B Luminescence Spectrometer the standard quinine sulfate solution in 0.01 M H_2SO_4, whose fluorescence quantum yield is known to be 0.54.

[(3,4,7,8-tetramethyl-1,10-phenanthroline-N-N')-bis-(2-(2,4-difluorophenyl)-5-(trifluoromethyl)pyridine-$C^{6'}$,N)-iridium (III)]hexafluorophosphate (UM01) (84%); ^{1}H NMR (300 MHz, $CDCl_3$) δ 8.51 (dd, J = 8.8, 2.4 Hz, 1H), 8.44 (s, 1H), 8.02 (dd, J = 8.9, 1.6 Hz, 1H), 7.95 (s, 1H), 7.41 (s, 1H), 6.75–6.65 (m, 1H), 5.74 (dd, J = 8.1, 2.3 Hz, 1H), 2.93 (s, 3H), 2.51 (s, 3H); MS (ES^+) m/z = 945.1627 (M^+-PF_6, 100).

[(3,4,7,8-tetramethyl-1,10-phenanthroline-N-N')-bis-(2-(2',4'-difluoro-phenyl)-1*H*-pyrazole-$C^{6'}$,N)-iridium (III)]hexafluorophosphate (UM02) (78%); ^{1}H NMR (300 MHz, $CDCl_3$) δ 8.36–8.31 (m, 2H), 8.09–8.03 (m, 1H), 6.86 (d, J = 2.5 Hz, 1H), 6.77–6.67 (m, 1H), 6.53–6.50 (m, 1H), 5.83 (dd, J = 8.3, 2.0 Hz, 1H), 2.88 (s, 3H), 2.48 (s, 3H); MS (ES^+) m/z = 787.1784 (M^+-PF_6, 100).

*corresponding author; e-mail: rukkiat_j@hotmail.com

The electroluminescence of iridium complex was dissolved in acetonitrile solution at a concentration of 12.5 mg ml^{-1}. Prior to the fabrication of the electroluminescence, the ITO glass substrates were thoroughly cleaned followed by UV-ozone treatment for 10 min. A thin film of poly(3,4-ethylenedioxythiophene):poly(styrenesulfonate) (PEDOT:PSS) layer was spin-coated at 3000 rpm for 180 s and baked at 260°C for 10 min. For the host-guest OLED device, the emitter layer was spin-coated with the host 2-(4-poly(9-vinylcarbazole) (PVK) and 2-(4-tert-butylphenyl)-5-(4-biphenylyl)-1,3,4-oxadiazole (PBD) in 3:1 w/w with the complex followed by 1,3,5-tris(2-N-phenylbenzimidazolyl)benzene (TPBi), LiF and aluminum cathode with a shadow mask under high vacuum. For simple LEC device, the complex films were spin-coated with or without 1-butyl-3-methylimidazolium (BMIM)PF_6 by varied the mole ratios and then capped with aluminum cathode. The electroluminescent properties of the resultant devices were performed using a Keithley 2400 source meter, as a power supply and multimeter, a Minolta LS-110, as a luminance detector, and an Ocean optics USB4000 spectrometer.

3. Results and discussions

The molecular structure of target charged iridium (III)complexes is depicted in Fig. 1. UM01 and

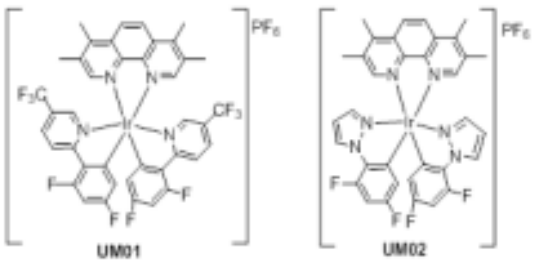

Fig. 1. The molecular structure of UM01 and UM02.

UM02 in dichloromethane (DCM) were characterized using UV-visible absorbance and fluorescence spectroscopy as shown in Fig. 2. The complex displays strong absorption bands between 250 and 300 nm which can be attributed to ligand-centered (LC) of the cyclometalated phenyl pyridine (ppy) and phenanthroline (phen). While, the weaker absorption bands about 400 nm and above can be assigned to metal- to-ligand charge transfer (MLCT). These characteristic are consistent with the previously reported in the literatures [13, 14]. The emission wavelengths of the both complexes were found around 480 nm which is compared to the blue-green color. We found that both UM01 and UM02 give the quantum yield of 0.01. We carried out DFT calculations to obtain the molecular geometries and electronic information of the charged iridium (III) complexes. The geometries of UM01 and UM02

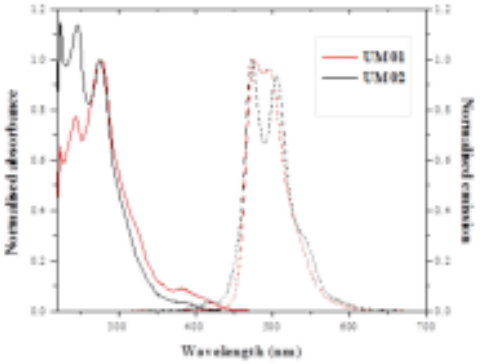

Fig. 2. UV-Vis absorption and emission of UM01 and UM02 in dichloromethane at room temperature.

were optimized at B3LYP/6-31G*:LANL2DZ. The frontier orbital and energy gap of UM02 are shown in Fig. 3 where the LUMO is located on the phenanthroline ligand and the HOMO involves the iridium and phenylene groups (Fig. 3). The calculated energy gap of UM02 shows a value at 3.37 eV which is in agreement with the result from photophysical experiments (3.10 eV).

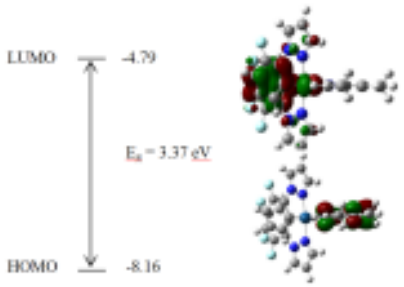

Fig. 3. HOMO and LUMO energies and corresponding orbital contours of UM02 by B3LYP/6-31G*:LANL2DZ. The E_g is defined as the HOMO-LUMO energy gap.

In order to evaluate the electroluminescent properties, complexes were first employed as emitting layer in both host-guest LECs [15] and OLEDs [16, 17] where PVK and PBD were mixed as the co-host. PEDOT:PSS acts as hole-injecting layer to facilitate electron transport. TPBi was used as an electron-transport/hole-blocking layer. Unfortunately, both host-guest LEC and OLED devices show weak current efficiency less than 0.2 cd A^{-1}. This can be explained by the unsuitable energy level of UM01 and host material [18]. Recently, the efficiency of the LECs devices can be improved by the addition of ionic liquid (IL) [19–21]. To investigate, we optimized the mole ratio of $BMIMPF_6$. We found that LEC structure: ITO/PEDOT:PSS/UM01:$BMIMPF_6$(1:1)/Al was the efficient device with a maximum brightness of 1.037 cd m^{-2} and a current efficiency of 1.14 cd A^{-1} (see Figure 4). With the same structure, we used UM02 as the emitter

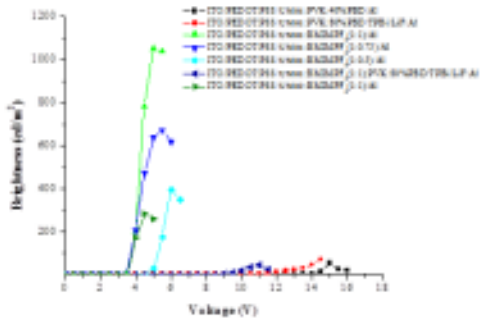

Fig. 4. Brightness versus voltage curves of the device based on UM01 and UM02 with a different structure.

TABLE I
LEC and OLED device performances of UM01 and UM02.

ITO/PEDOT: PSS/...	$V_{turn\ on}$ [V]	L_{max} [cdm^{-2}]	$\eta_{c\ max}$ [cd A^{-1}]	$\eta_{p\ max}$ [lm W^{-1}]	CIE (x,y)
...UM01: PVK:40%PBD/Al	13.5	52	0.04	0.01	N/A
...UM01: PVK:80%PBD/ TPBi/LiF/Al	10.6	70	0.12	0.03	N/A
...UM01: $BMIMPF_6$ (1:1)/Al	3.6	1037	1.14	0.80	0.23, 0.43
...UM01: $BMIMPF_6$ (1:0.75)/Al	3.5	670	0.68	0.48	0.24, 0.45
...UM01: $BMIMPF_6$ (1:0.5)/Al	4.5	396	0.49	0.26	0.24, 0.44
...UM01: $BMIMPF_6$(1:1): PVK:80%PBD/ TPBi/LiF/Al	8.6	44	0.08	0.03	N/A
...UM02: $BMIMPF_6$ (1:1)/Al	3.6	282	0.80	0.63	0.19, 0.40

in LECs. We found that the UM02 give a better blue CIE coordinate at 0.19, 0.40. However, the device shows a lower current efficiency of 0.08 cd A^{-1}. Detailed electroluminescent characteristics are summarized in Table I and Fig. 4.

Conclusions

The blue electroluminescence LECs can be achieved with the charged iridium (III) complexes. We found that the current efficiency can be improved to 1.14 cd A^{-1} by the addition of IL at 1:1 mole ratio into the emitting layer. The complex with C,N pyrazole ligand give a blue CIE coordination at 0.19, 0.40. Therefore, this research may be a useful and helpful data to develop an efficient real blue electroluminescence LECs in the future.

Acknowledgments

This work was financially supported by the Thailand Research Fund, the Higher Education Commission and Ubon Ratchathani University (MRG5480005). U. Mahanitipong thanks to YSTP and M. Srikaew thanks to SAST for the scholarships.

References

[1] K.K.-W. Lo, S.P.-Y. Li, K.Y. Zhang, *New J. Chem.* **35**, 265 (2011).

[2] Q. Zhao, S.-J. Liu, W. Huang, *Macromol. Rapid Commun.* **31**, 794 (2010).

[3] C. Ulbricht, B. Beyer, C. Friebe, A. Winter, U.S. Schubert, *Adv. Mater.* **21**, 4418 (2009).

[4] J.A.G. Williams, A.J. Wilkinson, V.L. Whittle, *Dalton Trans.*, 2081 (2008).

[5] M.S. Lowry, S. Bernhard, *Chem. Eur. J.* **12**, 7970 (2006).

[6] W.-Y. Wong, C.-L. Ho, *J. Mater. Chem.* **19**, 4457 (2009).

[7] C.D. Sunesh, G. Mathai, Y. Choe, *Org. Electron.* **15**, 667 (2014).

[8] U. Mitschke, P. Bäuerle, *J. Mater. Chem.* **10**, 1471 (2000).

[9] H.J. Bolink, L. Cappelli, S. Cheylan, E. Coronado, R.D. Costa, N. Lardies, M.K. Nazeeruddin, E. Ortı, *J. Mater. Chem.* **17**, 5032 (2007).

[10] M.K. Nazeeruddin, R.T. Wegh, Z. Zhou, C. Klein, Q. Wang, F. De Angelis, S. Fantacci, M. Grätzel, *Inorg. Chem.* **45**, 9245 (2006).

[11] L. He, L. Duan, J. Qiao, G. Dong, L. Wang, Y. Qiu, *Chem. Mater.* **22**, 3535 (2010).

[12] C. Rothe, C.-J. Chiang, V. Jankus, K. Abdullah, X. Zeng, R. Jitchati, A.S. Batsanov, M.R. Bryce, A.P. Monkman, *Adv. Funct. Mater.* **19**, 2038 (2009).

[13] F. De Angelis, S. Fantacci, N. Evans, C. Klein, S.M. Zakeeruddin, J.E. Moser, K. Kalyanasundaram, H.J. Bolink, M. Grätzel, M.K. Nazeeruddin, *Inorg. Chem.* **46**, 5989 (2007).

[14] A.B. Tamayo, S. Garon, T. Sajoto, P.I. Djurovich, I.M. Tsyba, R. Bau, M.E. Thompson, *Inorg. Chem.* **44**, 8723 (2005).

[15] L. He, L. Duan, J. Qiao, D. Zhang, L. Wang, Y. Qiu, *Org. Electron.* **11**, 1185 (2010).

[16] P. Wongkaew, U. Mahanitipong, N. Wongsang, S. Sahasithiwat, R. Jitchati, *e-J. Surf. Sci. Nanotech.* **12**, 141 (2014).

[17] H. Tang, Y. Li, Q. Chen, B. Chen, Q. Qiao, W. Yang, H. Wu, Y. Cao, *Dyes and Pigments* **100**, 79 (2014).

[18] W.S. Jeon, T.J. Park, S.Y. Kim, R. Pode, J. Jang, J.H. Kwon, *Org. Electron.* **10**, 240 (2009).

[19] L. He, L. Duan, J. Qiao, D. Zhang, G. Dong, L. Wang, Y. Qiu, *Synth. Met.* **166**, 52 (2013).

[20] S.T. Parker, J.D. Slinker, M.S. Lowry, M.P. Cox, S. Bernhard, G.G. Malliaras, *Chem. Mater.* **17**, 3187 (2005).

[21] H.-F. Chen, W.-Y. Hung, S.-W. Chen, T.-C. Wang, S.-W. Lin, S.-H. Chou, C.-T. Liao, H.-C. Su, H.-A. Pan, P.-T. Chou, Y.-H. Liu, K.-T. Wong, *Inorg. Chem.* **51**, 12114 (2012).